High-precision Numerical Scheme for Quantum Trajectories

by

Nattaphong Wonglakhon

Submitted to the Department of Physics, Faculty of Science
in partial fulfillment of the requirements for the degree of

Bachelor of Science in Physics

at the

MAHIDOL UNIVERSITY

June 2020

Author .....
Department of Physics, Faculty of Science
June 15, 2020

Certified by .....
Areeya Chantasri
Ph.D.
Thesis Supervisor

Certified by .....
Sujin Suwanna
Ph.D.
Thesis Supervisor

Accepted by .....
Asst.Prof. Kwan Arayathanitkul, Ph.D.
Head of the Department of Physics, Faculty of Science

High-precision Numerical Scheme for Quantum Trajectories

by

Nattaphong Wonglakhon

Submitted to the Department of Physics, Faculty of Science
on June 15, 2020, in partial fulfillment of the
requirements for the degree of
Bachelor of Science in Physics

Abstract

We propose a new completely positive measurement operator, which can improve the numerical precision in quantum trajectory simulations. For continuous measurements, the system's dynamics conditioned on diffusive measurement records can be described by the Itô stochastic master equation, which is sufficient for an infinitesimal time scale in quantum trajectory simulations. However, in real measurements, the time scale cannot be infinitesimal and the error from finite time steps is a key concern of this work. Currently, there are several approaches proposed to improve the precision error, namely, the Rouchon-Ralph approach [1], the Guevara-Wiseman approach [2], and the quantum Bayesian approach [3–6]. These approaches only satisfy necessary conditions for measurement operators only to lower order in the time scale. We therefore derive the new approach, the high-order completely positive map which gives the elegant measurement operator from the physical intuition, a quantum system coupled to a bosonic (harmonic oscillator) bath. This measurement operator (map) satisfies the completeness relation to the second order in $\mathrm{d}t$. The map also gives the unconditioned evolution which agrees with the second order in $\mathrm{d}t$ of the Lindblad master equation expansion. Furthermore, we also show numerical results that the high-order completely positive map yields the most accurate trajectories comparing with the other existing approaches.

Thesis Supervisor: Areeya Chantasri
Title: Ph.D.

Thesis Supervisor: Sujin Suwanna
Title: Ph.D.

Acknowledgments

Firstly, I would like to express my sincere gratitude to my advisors A. Chantasri and S. Suwanna for the continuous support during my difficult time of my study and research project. They have been motivating me to be patient and enthusiastic. Their guidance helped me in all the time of research and writing of this thesis. I could not have imagined having a better advisor and mentor for my undergraduate study.

Likewise my advisors, I would like to thank the rest of lecturers and staff officers in the department of physics, Mahidol University, for their encouragement and incredibly supportive documenting.

My sincere thanks also goes to Prof. Howard M. Wiseman, for offering me to visit the centre for quantum dynamics (CQD) at Griffith Univerisy, leading me working on diverse exciting projects, and providing me a lot of useful discussions.

I also acknowledge my friends and my colleagues who fulfil my university's life and my works at the laboratory, respectively.

I appreciate the Royal Government of Thailand scholarship (the Development and Promotion of Science and Technology Talents Project, DPST) for giving me the funding for my undergraduate study and visiting the CQD, Griffith University during summer in 2019.

Last but not the least, I would like to thank my family: my parents and my sisters, for the incredible support, even from six-hundred-kilometres distance.

Contents

List of Figures

List of Tables

List of Symbols

$\|\bullet\rangle$	Dirac ket
$\langle\bullet\|$	Dirac bra
$\mathrm{Tr}\{\bullet\}$	Trace functional
$\langle\bullet\rangle$	Expectation functional
ρ	Density matrix
$\mathcal{L}$	Lindblad superoperator
$\mathcal{D}$	Decoherence channel superoperator
$\mathcal{H}$	Backaction superoperator
$\hat{H}$	Hamiltonian operator
Ω	Rabi frequency
$\hat{U}$	Unitary operator
$\hat{c}$	Lindblad operator
$\hat{L}$	Lindblad operator of measured channel
$\hat{V}$	Lindblad operator of extra dephasing channel
$\hat{M}$	Measurement operator
$\wp_{\mathrm{ost}}$	Ostensible probability
$\hat{\sigma}_i$	Pauli Matrices $i = x, y, z$

$\hat{\sigma}_-$	Lowering operator
η	Measurement efficiency
$\mathrm{d}W$	Wiener increment
ξ	Gaussian white noise
D	Trace distance

Chapter 1

Introduction

An open quantum system has become an important concept in quantum measurements. In general, a quantum system can be measured by coupling it with a bath (or a measuring device) in order to study the system's evolution. The dynamics of an open quantum system can typically be derived from the Born-Markov approximation [7, 8]. The Born approximation is based on the assumption that the system of interest couples weakly to its bath. For the Markov approximation, this approximation is based on the idea that the interaction between the system and the bath is memoryless. In other words, the correlation time between the two is shorter than a time resolution dt for the system evolution. By tracing such the combined system over the bath's degree of freedom, we then obtain the unconditioned evolution of the system alone, which can be described by a master equation (ME) [7–11]. However, in the scenario that the bath's state is measured by a detection apparatus, the system dynamics should be conditioned on the measurement records, which leads to the "quantum trajectories" [7, 8]. This process is sometimes called "unraveling" the master equation. Furthermore, by summing over all the conditioned evolutions, or quantum trajectories, one can get back the Lindblad unconditioned evolution.

In this thesis, we consider a particular measurement called the continuous weak measurement, which is new concept different from the conventional projective measurement (collapsing style) that we leaned in the undergraduate level. For continuous measurements, the bath is observed continuously in time, giving stochas-

tic diffusive-type records. Therefore, the system's dynamics (quantum trajectories) evolves stochastically conditioned on the record realisations. The quantum trajectory for this case is usually described by the Itô stochastic master equation (Itô SME) [7, 8, 12, 13], where the stochasticity arises from the diffusive records. The Itô SME is a type of the stochastic differential equation, which can be solved by integration using an infinitesimal time step $\mathrm{d}t$.

There have been several experiments demonstrating the quantum trajectories, for example, quantum jumps and diffusive measurements in superconducting qubit experiments using microwave devices [2, 7, 12, 14–20], and the measurement of qubit's fluorescence from the atomic decay with emissions of photons [21, 22]. However, in real measurements, we cannot enforce the infinitesimal time scale as required by the SME. If the measurement is done with too small $\mathrm{d}t$, each step of the measurement record will not be independent of each other and the Markov assumption will be invalid. In this thesis, we therefore consider using maps (or measurement operators) to describe the system's dynamics, since they can used to be solve the dynamics with a small but finite time step $\mathrm{d}t$. To avoid the cumulative errors from the time resolution, the maps need to give accurate results to high order in $\mathrm{d}t$, in order to be used to describe the quantum trajectory. Moreover, the maps need to necessarily satisfy the completeness relation [7] and should agree with the Lindblad unconditioned evolution to high orders in $\mathrm{d}t$. This is to make sure that the trace preserving condition for the system's state does hold.

Quantum trajectories can be simulated by several approaches. The conventional Itô map is used to derive the SDE [7] works fine theoretically, but fails at solving valid quantum trajectories from experimental data because it satisfies the completeness relation only to the order $\mathcal{O}(\mathrm{d}t)$. The quantum Bayesian approach has been introduced to calculate the qubit trajectories in the quantum dots experiments [3–6]. In the recent work by Rouchon and Ralph, they proposed a way to implement the classical Euler-Milstein numerical scheme to the Itô SME for quantum trajectory [1, 23, 24], as an alternative approach for quantum feedback control [25]. However, the proposed map still only satisfies the completeness relation to $\mathcal{O}(\mathrm{d}t)$. The most recent work by

Guevara and Wiseman proposed a new map which satisfies the completeness relation to high order in dt and used them for the quantum state smoothing estimation [2, 26]. However, these maps still does not agree with the Lindblad unconditioned state expanded to $\mathcal{O}(\mathrm{d}t^2)$ derived by Steinbach *et al.* in Ref. [16].

In this thesis, we aim to propose the new measurement operator (map) which satisfies our criterions (1) satisfies the completeness relation to second order in dt, and (2) the unconditioned state in agreement with the expansion of the Lindblad master equation to second order in dt. We also show numerical simulation results from the qubit z-measurement and make the comparison among different approaches using the trace distance.

This thesis is organised as follows. In the next chapter, Chapter 2, we briefly review the background knowledge about the open quantum system and quantum measurement theory. We review two cases of the system's evolution which are unconditioned and conditioned evolution. The unconditioned evolution can be derived by tracing out over all the bath's degree of freedoms. On the other hand, the conditioned evolution or quantum trajectory is constructed from the continuous measurement record which is related to a stochastic process. Moreover, we also review the dephasing or decoherence effects which are the relevant processes in open quantum systems.

In Chapter 3, we review the four existing approaches, which are the Itô map, the Rouchon-Ralph approach, and the Guevara-Wiseman map. We show the calculations of the completeness relation and the unconditioned state evolution.

In Chapter 4, this chapter we derive our proposed high-order completely positive map from the system (qubit) bosonic-bath coupling. We first derive the map for a simple system which has a single measured channel, and the system's Hamiltonian is set to be zero ($\hat{H} = 0$). We then relax that constraint and add the system's Hamiltonian and the multiple unmeasured dephasing channels. Lastly, we give the examples, the map for the qubit z-measurement and the measurement of the qubit's fluorescence.

In Chapter 5, we explain the numerical simulation we use for an example of the

z-measurement of superconducting qubit experiments. We first explain the basic idea of such experiment briefly. Then, in the simulation section, we generate the true measurement records in order to use to simulate quantum trajectories for the different approaches. We end this chapter by showing the comparison among four approaches which are the Itô map, the Rouchon-Ralph approach, the high-order completely positive map, and the quantum Bayesian approach.

Finally, we finish our thesis with the conclusion chapter, which also includes a discussion about the simulation results.

Chapter 2

Background

This chapter is organised as follows. We first explain the concept of quantum states for a single qubit, which is represented by a 2×2 density matrix and will be used throughout this thesis. In Section 2.2, we review the idea of the open quantum system, which is an important concept in quantum measurement as the system of interest has to be coupled with a bath state. In the next section, Section 2.3, we show the idea of the operations to describe the time evolution of the quantum state for an open quantum system. The evolution of the quantum state can be considered in two scenarios, namely, the unconditioned evolution and conditioned evolution. In Section 2.4, the unconditioned evolution, it describes the evolution of the quantum state in the case that we have no information about the bath's state by tracing out the combined system over its bath degree of freedom obtaining the Lindblad master equation. However, in the scenario that we have information about the bath's state, we can unravel the master equation which finally obtain the conditioned evolution. In Section 2.5, we review the conditioned evolution which can be done by a measurement operation. In this thesis, we focus on the continuous weak measurement in Section 2.6 which is associated with the stochastic process. In Section 2.7, we review the idea of the stochastic process, we then go on to the quantum trajectory in Section 2.8, which describes the qubit evolution stochastically. Finally, we end up this chapter with the dephasing processes in Section 2.9, we investigate the T_1 and T_2 dephasings which occur in the open quantum system.

2.1 Quantum State

In quantum computing, a qubit or a quantum bit is a two-level system, which can be realised on many physical platforms. For example, in a spin 1/2 particle, a qubit can be constructed from the spin state of an electron, where the two states correspond to the spin up and spin down. Regardless of a physical platform, a quantum mechanical state of a two-level system can be expressed as a 2×2 matrix, called a *density matrix* or a *density operator*. In terms of the Pauli matrices, a density matrix can be written as

$$\rho = \frac{1}{2}(\hat{1} + x\hat{\sigma}_x + y\hat{\sigma}_y + z\hat{\sigma}_z) = \frac{1}{2}(\hat{1} + \vec{r} \cdot \hat{\sigma}), \tag{2.1}$$

where $\vec{r} = (x, y, z)$ is called a Bloch vector, and $\hat{\sigma} = (\hat{\sigma}_x, \hat{\sigma}_y, \hat{\sigma}_z)$ is a vector whose entries are Pauli matrices. The general properties of the density operator are

1. ρ has trace equal to one i.e., $\mathrm{Tr}[\rho] = 1$ (trace condition) .

2. ρ is a positive operator i.e., $\langle\varphi|\rho|\varphi\rangle \geqslant 0$ (positivity conditon) .

2.2 Open Quantum System

Open quantum systems are quantum systems that interact with their environment or bath. The usual treatment is to consider a combined system (a quantum system of interest and the bath) as a closed system evolving unitarily. One can then trace out the bath's degrees of freedom to obtain a reduced dynamics of the quantum system of interest. However, the system's dynamics is also strongly dependent on whether there exists any observation of the bath. In the case where the bath is measured, the system's dynamics will be affected, as a result of measurement backaction.

Considering a combined system which has its state living in a tensor product of Hilbert spaces $\mathcal{H}_s \otimes \mathcal{H}_e$, where $\mathcal{H}_s$ and $\mathcal{H}_e$ are the Hilbert spaces of the system of interest and its bath, respectively. Using the Born-Markov assumption, we can write the combined system's state ϱ as initially prepared as a product state $\varrho = \rho \otimes \rho_e$

[7, 10, 11] (the weak coupling from the Born approximation). In this work, we are interested in the continuous observation of the bath; therefore, we will investigate the time evolution of such combined system during an infinitesimal time $\mathrm{d}t$. Let the dynamics of the combined system be described by a unitary map $\mathcal{U}_{\mathrm{d}t}[\bullet] = \hat{U}_{t+\mathrm{d}t,t} \bullet \hat{U}^{\dagger}_{t+\mathrm{d}t,t}$ mapping the combined state from time t to $t + \mathrm{d}t$. Assuming that the state of the bath at time t is set as one of its eigenstate, i.e., $\rho_e(t) = |e_0\rangle \langle e_0|$ (using $|e_k\rangle$ as the bath's eigenstates) [10], we can write the combined system's dynamics as,

$$\varrho(t + \mathrm{d}t) \quad = \quad \hat{U}_{t+\mathrm{d}t,t}(\rho_t \otimes |e_0\rangle \langle e_0|)\hat{U}^{\dagger}_{t+\mathrm{d}t,t}, \tag{2.2}$$

where ρ_t is the system's state at time t.

After the evolution in Eq. (2.2), the system become entangled with the bath. In the regime where the bath's state is not observed, or equivalently no information available about the bath's state after the interaction, the reduced density matrix for the system's state can be found by taking a trace over the bath's degree of freedom, resulting in the *decoherence* (non-unitary evolution) [7, 10, 11, 27] on the system's state. The decoherence can be thought of as a result of noises from the bath affecting the system. However, in the case where there is an observation, i.e., the bath's state is measured by some measurement detection scheme, then the system's state should reflect the information gained from measuring the bath. We will see more discussions on the conditioned evolution in Sections 2.5 and Chapter 3.

2.3 Superoperators and Operations

An open quantum system requires a definition of a superoperator, which describes a change in a quantum state. In this case, the quantum state evolves continuously in time, so the superoperator map will be defined for the infinitesimal time step. In general, we can define a superoperator to map the density matrix as

$$\rho \to \rho' \quad = \quad \mathcal{M}\rho, \tag{2.3}$$

where the superoperator $\mathcal{M}$ is on the space of Hilbert-space operators and must satisfy the following identities. [7]

- $\mathcal{M}$ has to be trace-preserving. That is, for any ρ, $0 \leq \mathrm{Tr}[\mathcal{M}\rho] \leq 1$.

- $\mathcal{M}$ has to be a linear map operator, giving

$$\mathcal{M}\sum_j \wp_j \rho_j \quad = \quad \sum_j \wp_j \mathcal{M}\rho_j. \tag{2.4}$$

- $\mathcal{M}$ has to be completely positive. Completely positive operations map positive operators to positive operators,

$$\mathcal{M} : \rho \geq 0 \quad \rightarrow \quad \rho' = \mathcal{M}\rho \geq 0. \tag{2.5}$$

  If we consider an extra arbitrary subsystem R coupling with the subsystem Q, we can write a map of the form $\mathcal{I}_R \otimes \mathcal{M}_Q$ for the combined system RQ also, which has to also be completely positive,

$$\mathcal{I}_R \otimes \mathcal{M}_Q : \rho_{RQ} \geq 0 \quad \rightarrow \quad \rho'_{RQ} = (\mathcal{I}_R \otimes \mathcal{M}_Q)\rho_{RQ} \geq 0. \tag{2.6}$$

The superoperator $\mathcal{M}$ is said to be a quantum operation if it satisfies these three identities. An operation has the sum representation or the Kraus representation,

$$\mathcal{M}(\rho) \quad = \quad \sum_j \hat{M}_j \rho \hat{M}_j^\dagger, \tag{2.7}$$

where $\hat{M}_j$ is a Kraus operator which satisfies

$$\hat{1} - \sum_j \hat{M}_j^\dagger \hat{M}_j \geq 0. \tag{2.8}$$

2.4 Unconditioned Evolution

As we mentioned earlier, the system's dynamics alone can be obtained without conditioning on any measurement result by tracing out the bath's degree of freedom, we then get the unconditioned dynamics. From Eq. (2.2), we can write that the system's state is given by

$$\rho(t+\mathrm{d}t) \;=\; \mathrm{Tr}_{\mathrm{e}}\left[\hat{U}_{t+\mathrm{d}t,t}(\rho_t\otimes|e_0\rangle\langle e_0|)\hat{U}^{\dagger}_{t+\mathrm{d}t,t}\right], \tag{2.9}$$

where the trace $\mathrm{Tr}_{\mathrm{e}}[\cdots]\equiv\sum_k\langle e_k|\cdots|e_k\rangle$ is defined for the basis states of the bath's Hilbert space. Under the Born-Markov assumption, one finds that the reduced system's dynamics Eq. (2.9) can be written in the form [7],

$$\rho(t+\mathrm{d}t) \;=\; e^{\mathrm{d}t\mathcal{L}}\rho(t), \tag{2.10}$$

where

$$\mathcal{L}\bullet = -i[\hat{H},\bullet]+\sum_{j=1}^{N}\mathcal{D}[\hat{c}_j]\bullet, \tag{2.11}$$

is the Lindblad superoperator. Here we define $\hat{H}$ as a Hermitian operator describing the unitary dynamics of the system's state and $\hat{c}_j$ as the Lindblad operators. The superoperator $\mathcal{D}$ describes all decoherence channels defined as $\mathcal{D}[\hat{c}]\bullet=\hat{c}\bullet\hat{c}^{\dagger}-\frac{1}{2}\{\hat{c}^{\dagger}\hat{c},\bullet\}$, noting that we have taken $\hbar=1$ throughout the thesis.

The Lindblad increment evolution Eq. (2.10) can be solved in the time-continuum limit, $\mathrm{d}t\to 0$, where one can expand the exponential superoperator to first order in $\mathrm{d}t$,

$$\rho(t+\mathrm{d}t) \;=\; \rho(t)+\mathrm{d}t\mathcal{L}\rho(t), \tag{2.12}$$

giving the usual Lindblad master equation $\partial_t\rho=\mathcal{L}\rho(t)$ [28]. However, in the scenario where one has to solve Eq. (2.10) with a finite $\mathrm{d}t$, we need to expand the exponential

to higher orders in dt for a more accurate result.

Let us first consider equations with a single Lindblad operator $\hat{c}$ and no unitary dynamcis $\hat{H} = 0$, in order to focus on the dynamics from measured and unmeasured decoherence channels. By performing the Taylor expansion, on Eq. (2.10) we obtain the result up to second order in dt derived by Steinbach *et al.* in Ref.[16], which gives

$$\begin{aligned} \rho(t + \mathrm{d}t) &= \left(1 + \mathrm{d}t\mathcal{L} + \tfrac{1}{2}\mathrm{d}t^2\mathcal{L}^2\right)\rho(t), \\ &= \rho(t) + \mathcal{D}[\hat{c}]\rho(t)\mathrm{d}t + \tfrac{1}{2}\mathcal{D}[\hat{c}]\big[\mathcal{D}[\hat{c}]\rho(t)\big]\mathrm{d}t^2, \end{aligned} \tag{2.13}$$

where we have used

$$\begin{aligned} \mathcal{D}[\hat{c}]\big[\mathcal{D}[\hat{c}]\rho(t)\big] = \tfrac{1}{4}\big[\rho(t)(\hat{c}^\dagger\hat{c})^2 + (\hat{c}^\dagger\hat{c})^2\rho(t)\big] + \tfrac{1}{2}\hat{c}^\dagger\hat{c}\rho(t)\hat{c}^\dagger\hat{c} - \tfrac{1}{2}\big[\hat{c}\rho(t)(\hat{c}^\dagger)^2\hat{c} + \hat{c}^\dagger\hat{c}^2\rho(t)\hat{c}^\dagger\big] \\ - \tfrac{1}{2}\big[\hat{c}\rho(t)\hat{c}^\dagger\hat{c}\hat{c}^\dagger + \hat{c}\hat{c}^\dagger\hat{c}\rho(t)\hat{c}^\dagger\big] + \hat{c}^2\rho(t)(\hat{c}^\dagger)^2. \end{aligned} \tag{2.14}$$

We will use this expansion later in Chapter 3 to check properties of measurement operations.

2.5 Measurement Backaction and Conditioned Evolution

Let us consider a scenario that one acquires information about the system by measuring the state of the bath; for example, by collapsing the detector's state to $|e_d\rangle$ which gives a measurement outcome d. We can unravel the Lindblad master equation in Eq. (2.12) and obtain the system's state conditioned on measurement records. One can project the combined system's state onto $|e_d\rangle$ and then trace out the bath degree of freedom. This gives the conditioned reduced system's state ρ_d as (d indicates for the conditioned state)

$$\rho_d(t + \mathrm{d}t) \propto \mathrm{Tr}_e\{|e_d\rangle\langle e_d|\,\varrho(t)\} = \hat{M}_d\rho(t)\hat{M}_d^\dagger, \tag{2.15}$$

where $\hat{M}_d = \langle e_d | \hat{U}_{t+\mathrm{d}t,t} | e_0 \rangle$ is a measurement operator. To get the normalised form, we divide Eq. (2.15) by its trace, giving

$$\rho_d(t+\mathrm{d}t) \quad = \quad \frac{\hat{M}_d \rho(t) \hat{M}_d^\dagger}{\mathrm{Tr}\left[\hat{M}_d \rho(t) \hat{M}_d^\dagger\right]}. \tag{2.16}$$

Noting that the normalisation factor in Eq. (2.16) is the probability of getting the measurement outcome d given the state $\rho(t)$, which is

$$\wp(d|\rho(t)) \quad = \quad \mathrm{Tr}\left[\hat{M}_d \rho(t) \hat{M}_d^\dagger\right]. \tag{2.17}$$

Let us now consider the unconditioned evolution again. We can obtain the unconditioned evolution from summing over all the measurement outcomes k. That is

$$\rho(t+\mathrm{d}t) \quad = \quad \mathrm{Tr}_e[\varrho(t)] = \sum_k \hat{M}_k \rho(t) \hat{M}_k^\dagger, \tag{2.18}$$

which coincides with the expression in Eq. (2.10),

$$\rho(t+\mathrm{d}t) \quad = \quad e^{\mathrm{d}t\mathcal{L}} \rho(t) = \sum_k \hat{M}_k \rho(t) \hat{M}_k^\dagger. \tag{2.19}$$

Here, we have left the dominator of Eq. (2.19), which should be its trace. This is because the norm is equal to 1 to preserve the total probability. Consequently, the measurement operator must satisfy the completeness relation,

$$\sum_k \hat{M}_k^\dagger \hat{M}_k = \hat{1}, \tag{2.20}$$

which is one of the important properties of the measurement operator we consider in this work. For continuous measurement outcomes, we can check the completeness relation by replacing the sum with an integral over all possible continuous-value relevant.

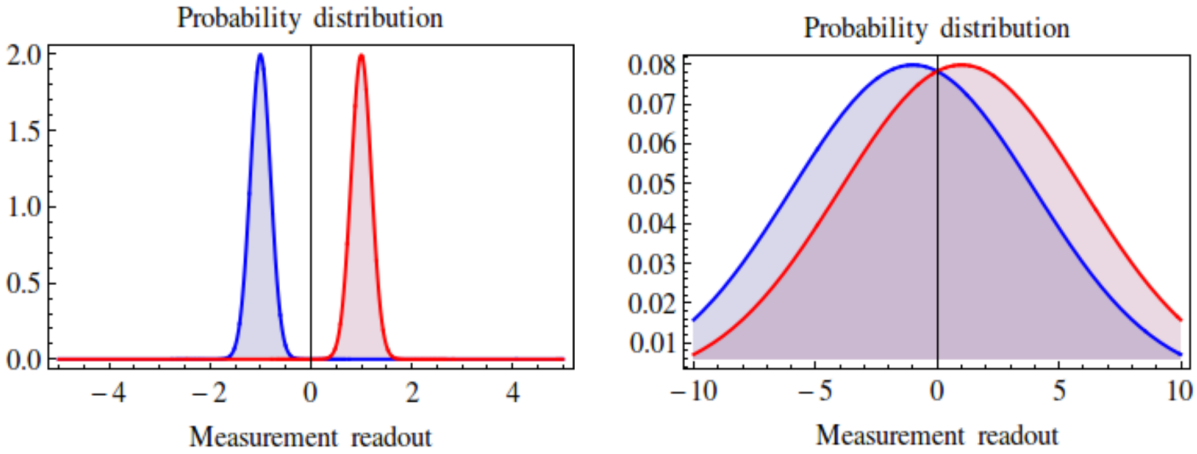

Figure 2-1: This figure [29] displays the probability distribution of the measurement readout of a qubit measurement in z-basis (blue lines for $|0\rangle$ and red lines for $|1\rangle$). (Left) Strong (projective) measurement. (Right) Weak measurement.

2.6 Continuous Weak Measurement

Quantum continuous weak measurements is a new concept different from the projective (strong) measurement which assumes a collapse of the state of the measured system to an eigenstate of the measured observable. In this section, we use an example of a measurement of a Hermitian observable ($\hat{\sigma}_z$) and compare between its strong measurement and its weak measurement.

We showed in the previous section how the measurement operator plays a role in the quantum measurement theory. The measurement operator describes how the state of the system changes (backaction) as a result of a measurement. Let us consider the strong measurement. If one measures the system with a projective measurement, such system will collapse to an eigenstate of the measured observable. If one were to repeat the measurement again, the system state will remain unchanged. However, for the weak measurement, the system evolution can gradually change as in Eq. (2.15). By measuring the system continuously in time, we can track the continuing evolution of the system's state.

For a measurement of a Hermitian observable, one can see the difference of both measurement styles by looking the distribution of the measurement readouts as in Figure 2-1. For a strong measurement, the variance of the readout's distribution is

small compared to that of the weak measurement. For the latter, one obtain less information of the system, since the overlaping area of both measurement readouts is large. That is, given a measurement result somewhere in the overlapped area, we cannot say exactly which eigenstate the state has collapsed to. The state is then some superposition of possible eigenstates. Moreover, the broad distribution indicates that the measurement results are random numbers, which will simulate a stochastic process in time. We are going to investigate this in more detail in the next section.

2.7 Relevant Theories from Classical Stochastic Process

In this section, we briefly review two concepts of stochastic differential equations (SDEs). One is the conventional Itô SDE and another is the Euler-Milstein scheme. The stochastic process describes a time evolution which contains a stochastic element, i.e., the Wiener increment $\mathrm{d}W$. The properties of the Wiener process are the zero mean, $\langle \mathrm{d}W(t) \rangle = 0$ and its variance proportional to $\mathrm{d}t$, $\langle \mathrm{d}W^2 \rangle \sim \mathrm{d}t$. We also show the Euler-Milstein technique, which is the extension of the Itô SDE for high order in $\mathrm{d}W$.

2.7.1 Itô SDEs

Given a system's variable of interest x, an Itô stochastic differential equation can be written generally in the time continuous form

$$\mathrm{d}x \;=\; f(x)\mathrm{d}t + \sum_{r}^{m} g_r(x)\mathrm{d}W_r, \tag{2.21}$$

where $f(x)$ and $g_r(x)$ are arbitrary functions, and $\mathrm{d}W_r$ is a Gaussian Wiener increment. The sum is over all m noises that affect the system. We can also define a Gaussian white noise from the wiener process as $\xi(t) = \mathrm{d}W/\mathrm{d}t$, which satisfies the

following identities [7, 14, 30],

$$\langle \xi(t) \rangle = 0, \tag{2.22a}$$

$$\langle \xi^2(t) \rangle = 1/\mathrm{d}t, \tag{2.22b}$$

$$\langle \xi(t)\xi(t') \rangle = \delta(t - t'), \tag{2.22c}$$

where $\langle \bullet \rangle$ is the expectation value over all realisations of $\xi(t)$. Noting that we can interpret Eqs. (2.22) as a Gaussian white noise with zero mean, $1/\mathrm{d}t$ variance. Moreover, the noises at different time steps are independent of each other (which is a result of the Markovian assumption). The Itô SDE Eq. (2.21) is valid when $\mathrm{d}t$ is infinitesimal, and thus the dynamics can be obtained by using only the first order in $\mathrm{d}W$.

2.7.2 Euler-Milstein Scheme

The Euler-Milstein scheme [23] is the technique to improve the accuracy of the Itô SDE by adding terms with high order in $\mathrm{d}W$. We will here show the final result and leave the detailed derivation in Appendix A. Let us write equations in the time-discrete form. The Euler-Milstein scheme for the Itô SDE in Eq. (2.21) is given by the numerical scheme as

$$x_{n+1} = x_n + f(x_n)\Delta t + \sum_{r=1}^{m} g_r(x_n)\Delta W_{r,n} + \sum_{r,s=1}^{m} \frac{\partial g_s(x_n)}{\partial x} \cdot g_r(x_n)\left(\frac{\Delta W_{r,n}\Delta W_{s,n} - \delta_{r,s}\Delta t}{2}\right), \tag{2.23}$$

where $f(x)$ and $g_r(x)$ are the same as in Eq. (2.21). This equation can give a more precise dynamics of x than the Itô SDE, where Δt is not small enough.

2.8 Quantum Trajectories

Now that we have introduced the stochastic process, we can write the conditioned evolution Eq. (2.16) in the $\mathrm{d}t \to 0$ limit. This gives a SDE for quantum states, which describes a quantum trajectory. A quantum trajectory refers to a path for a quantum's system state, which behaves stochastically because it is conditioned on measurement records. In quantum weak measurements, there have been several experiments demonstrating the quantum's dynamics, especially, using the homodyne and heterodyne detections [7, 8, 12, 13]. Let us consider a diffusive homodyne detection. The information of the measurement readouts (via a measurement operator in Eq. (2.16)) leads to the stochasticity in the system's state. Here, we can describe the system's dynamics by a stochastic master equation [7],

$$\frac{\mathrm{d}\rho}{\mathrm{d}t} = -i[\hat{H},\rho] + \sum_{\mu}\mathcal{D}[\hat{V}_{\mu}]\rho + \sum_{r}\mathcal{D}[\sqrt{\eta_r}\hat{L}_r]\rho + \sum_{r}\sqrt{\eta_r}\big(\mathcal{H}[\hat{L}_r]\rho\big)\frac{\mathrm{d}W_r}{\mathrm{d}t}, \qquad (2.24)$$

where $\hat{H}$ is the system's Hamiltonian and a superoperator $\mathcal{H}$ is defined as $\mathcal{H}[\hat{A}]\rho = \hat{A}\rho + \rho\hat{A}^{\dagger} - \mathrm{Tr}\Big[\hat{A}\rho + \rho\hat{A}^{\dagger}\Big]\rho$. $\mathrm{d}W_r$ is a Wiener increment as defined earlier, and η_r are detection efficiencies ($\eta_r \in [0,1]$). $\hat{L}_r$ and $\hat{V}_{\mu}$ are Lindblad operators describing the coupling channels between the system and the baths. We separate the decoherence channels, $\hat{L}_r$ from the measured channels, $\hat{V}_r$ from unmeasured channels.

2.9 Decoherence Effects on Qubits

Performing a measurement can give rise to the dephasing since the system interacts with its bath. The decoherence channels used in this thesis include the unmeasured channels (from measurement inefficiency), the T_1 spin relaxation, and the T_2 dephasing. The T_1 and T_2 processes are from the spontaneous emission of photons and the error of the qubit's phase, respectively.

2.9.1 T_1 spin relaxation

This decoherence occurs from the spontaneous emission of photons. The state of a quatum system can naturally decay to its ground state. For a two-level (qubit) system, we denote the atomic ground and excited states as $|\mathrm{g}\rangle$ and $|\mathrm{e}\rangle$, respectively. Let us define the state of the bath as the state of the detection of an emitted photon. If the atomic decay occurs, the state of the bath is in $|1\rangle$ (one photon is presented). On the other hand, if there is no atomic decay, the state of the bath is in $|0\rangle$ (the vacuum state).

Here, we can define the Kraus operators for both processes as $\hat{M}_1$ and $\hat{M}_0$ describe the evolution of the decay to the ground state (*quantum jump*) and the evolution of *no-jump* state, respectively. There is a probability p that the excited state decays to the ground state, giving

$$\begin{aligned} |\mathrm{g}\rangle|0\rangle &\rightarrow |\mathrm{g}\rangle|0\rangle, \\ |\mathrm{e}\rangle|0\rangle &\rightarrow \sqrt{1-p}\,|\mathrm{e}\rangle|0\rangle + \sqrt{p}\,|\mathrm{g}\rangle|1\rangle. \end{aligned} \tag{2.25}$$

Therefore, we can make sense of the Kraus operators for no-jump $\hat{M}_0$ and jump $\hat{M}_1$ [10], which are given by

$$\hat{M}_0 = \begin{pmatrix} \sqrt{1-p} & 0 \\ 0 & 1 \end{pmatrix}, \tag{2.26}$$

$$\hat{M}_1 = \begin{pmatrix} 0 & 0 \\ \sqrt{p} & 0 \end{pmatrix}, \tag{2.27}$$

where $\hat{M}_k = \langle k|\,\hat{U}\,|0\rangle$ under the unitary evolution of this process $\hat{U} = \exp\left\{\hat{a}^\dagger\hat{b} - \hat{a}\hat{b}^\dagger\right\}$, where $\hat{a}, \hat{b}$ and $\hat{a}^\dagger, \hat{b}^\dagger$ are annihilation and creation operators.

We can derive the decoherence process from the sum-representation as in Eq. (2.7). The T_1 process happens when there is the spontaneous emission, but we do not know

when the photon is emitted as there is no detection. Let us define the qubit state as

$$\rho = \begin{pmatrix} \rho_{ee} & \rho_{eg} \\ \rho_{ge} & \rho_{gg} \end{pmatrix},$$

the density matrix map for the T_1 process becomes,

$$\begin{aligned} \mathcal{M}(\rho) &= \rho' = \hat{M}_0 \rho \hat{M}_0^\dagger + \hat{M}_1 \rho \hat{M}_1^\dagger, \\ &= \begin{pmatrix} \rho_{ee} + p\rho_{gg} & \sqrt{1-p}\rho_{eg} \\ \sqrt{1-p}\rho_{ge} & (1-p)\rho_{gg} \end{pmatrix}. \end{aligned}$$

Assuming that the probability of the transition during the time interval δt is $p = \Gamma_1 \delta t$, where Γ_1 is the decay rate of this process. If we apply the channel repeatedly n times which the total time is $t = n\delta t$, then the coefficients of the off-diagonal elements can be evaluated as $(1-p)^{n/2} \approx e^{-\Gamma_1 t/2}$, as well as $(1-p)^n$, it can be evaluated as $e^{-\Gamma_1 t}$. In the scenario that we take the limit $t \to \infty$, the off-diagonal and the excited elements converge to zero. Consequently, the ground state element converges to one, obtaining the density matrix as

$$\rho' = \begin{pmatrix} 0 & 0 \\ 0 & 1 \end{pmatrix}, \tag{2.28}$$

which show that the atom finally decays to the ground state. In general, T_1-dephasing relates to the lowering operator $\hat{\sigma}_-$. The Lindblad operator for this process is

$$\hat{V}_1 = \frac{1}{\sqrt{\Gamma_1}} \hat{\sigma}_-, \tag{2.29}$$

where $\hat{\sigma}_-$ is defined as $\hat{\sigma}_- = (\hat{\sigma}_x - i\hat{\sigma}_y)/2$.

2.9.2 T_2 dephasing

This process can be thought of coming from the random phase of a qubit, as a result of a fluctuation in the qubit's frequency. Usually in an experiment, the qubit's frequency can be measured by using the Ramsey fringe experiment. However, there can still be noises that affect the frequency which are undetected. Let the qubit rotate about the z-axis of Bloch sphere with a frequency ω, leading to the Hamiltonian $\hat{H} = \frac{\omega}{2}\hat{\sigma}_z$. The qubit evolution under the unitary operator $U = e^{-i\phi\hat{\sigma}_z/2}$, where $\phi = \omega\delta t$, is given by

$$\rho(t+\delta t) = \begin{pmatrix} \rho_{ee} & e^{-i\phi}\rho_{eg} \\ e^{i\phi}\rho_{ge} & \rho_{gg} \end{pmatrix}. \tag{2.30}$$

We assume that the fluctuation of the qubit phase follows the Gaussian stochastic process, where its distribution is given by $g(\phi) \propto e^{-\phi^2/(2\sigma^2)}$. We here average over all the qubit's phase, giving

$$\rho(t+\delta t) = \begin{pmatrix} \rho_{ee} & \Gamma_2\rho_{eg} \\ \Gamma_2^*\rho_{ge} & \rho_{gg} \end{pmatrix}, \tag{2.31}$$

where $\Gamma_2 = \langle e^{-i\phi} \rangle = \int \mathrm{d}\phi g(\phi) e^{i\phi} = e^{-\sigma^2/2}$ is an exponential decay. If we define the dephasing rate γ, we can see that $\sigma^2 = 2\gamma\delta t$. We can also write,

$$\begin{aligned} \rho(t+\delta t) &= \int \mathrm{d}\phi g(\phi) e^{-i\phi/2\hat{\sigma}_z}\rho e^{i\phi/2\hat{\sigma}_z}, \qquad (2.32) \\ &= \int \mathrm{d}\phi g(\phi)\big(\cos^2(\phi/2)\rho + \sin^2(\phi/2)\hat{\sigma}_z\rho\hat{\sigma}_z - i\cos(\phi/2)\sin(\phi/2)[\hat{\sigma}_z,\rho]\big). \end{aligned}$$

Since the distribution of the qubit's phase is a symmetric distribution and normalisable, then the last term vanishes (odd integration), giving

$$\rho(t+\delta t) = (1-p)\rho + p\hat{\sigma}_z\rho\hat{\sigma}_z, \tag{2.33}$$

where $p = \int \mathrm{d}\phi g(\phi) \sin^2(\phi/2) = \int \mathrm{d}\phi g(\phi) \big(\frac{1-\cos(\phi)}{2}\big) = \frac{1-\Gamma_2}{2}$. We rewrite Eq. (2.33), to get

$$\rho(t+\delta t) \;=\; \big(\frac{1+\Gamma_2}{2}\big)\rho + \big(\frac{1-\Gamma_2}{2}\big)\hat{\sigma}_z\rho\hat{\sigma}_z. \tag{2.34}$$

We perform the Taylor expansion of Γ_2 by considering a small δt, giving that $\Gamma_2 = e^{-\gamma\delta t} = 1 - \gamma\delta t$. Then substitute Γ_2 in Eq. (2.34), we have

$$\begin{aligned} \rho(t+\delta t) &= \rho + \frac{\gamma}{2}\delta t\big[\hat{\sigma}_z\rho\hat{\sigma}_z - \frac{1}{2}\big(\rho\hat{\sigma}_z^2 + \hat{\sigma}_z^2\rho\big)\big] \\ &= \rho + \mathcal{D}[\sqrt{\gamma/2}\hat{\sigma}_z]\rho\delta t. \end{aligned} \tag{2.35}$$

Therefore, the Lindblad operator of this process is

$$\hat{V}_2 \;=\; \sqrt{\frac{\gamma}{2}}\hat{\sigma}_z. \tag{2.36}$$

Chapter 3

Existing Approaches

Currently, there have been several approaches proposed to unravel the Lindblad master equation. We can represent each approach by an associated measurement operation, which we will call it a "map". In this chapter, we will review these approaches including the conventional Itô map, the map adapted from the Euler-Milstein approach, and the completely positive map proposed by Guevara and Wiseman [2]. As we mentioned in Section 2.5, the measurement operator should satisfy the completeness relation Eq.(2.20) and should lead to the unconditioned state described by the Lindbald master equation as in Eq. (2.19), after summing over all possible measurement results. In this thesis, we only consider diffusive unraveling. For the clarity of the derivation in this section, we consider a single Lindblad operator $\hat{c}$ with taking the system's Hamiltonian to be $\hat{H} = 0$. We then show the calculation for the completeness relation and then show the unconditioned state comparing with the high order expansion of the Lindblad master equation for the three approaches.

3.1 Conventional Itô Map

This approach starts with the Itô stochastic master equation in Eq. (2.24). Considering the Itô rule $\mathrm{d}W^2 \sim \mathrm{d}t$, we can write a measurement operator for the Itô SME

[7] as

$$\hat{M}_{\rm I}(y_t) \;=\; \hat{1} - \tfrac{1}{2}\hat{c}^\dagger\hat{c}{\rm d}t + \hat{c}y_t{\rm d}t, \tag{3.1}$$

where $y_t = {\rm Tr}\left[\hat{c}\rho + \rho\hat{c}^\dagger\right] + {\rm d}W/{\rm d}t$ is a measurement readout. We can get back the Itô SME by calculating $\rho(t+{\rm d}t) = \hat{M}_{\rm I}\rho(t)\hat{M}_{\rm I}^\dagger/\,{\rm Tr}\left[\hat{M}_{\rm I}\rho(t)\hat{M}_{\rm I}^\dagger\right]$, taking limit ${\rm d}t \to 0$. We then perform the calculation to check its completeness relation and the Lindblad master equation to second order in ${\rm d}t$ as follows.

- Completeness relation:

$$\int {\rm d}y_t \wp_{\rm ost}\hat{M}_{\rm I}^\dagger(y_t)\hat{M}_{\rm I}(y_t) \;=\; \hat{1} + \frac{1}{4}\left(\hat{c}^\dagger\hat{c}\right){\rm d}t^2 + \mathcal{O}({\rm d}t^3) \tag{3.2}$$

- Lindblad master equation:

$$\begin{aligned}\rho(t+{\rm d}t) \;&=\; \int {\rm d}y_t \wp_{\rm ost}\hat{M}_{\rm I}(y_t)\rho(t)\hat{M}_{\rm I}^\dagger(y_t) \\ &=\; \rho(t) + \mathcal{D}[\hat{c}]\rho(t){\rm d}t + \frac{1}{4}\hat{c}^\dagger\hat{c}\rho(t)\hat{c}^\dagger\hat{c}{\rm d}t^2 + \mathcal{O}({\rm d}t^3)\end{aligned} \tag{3.3}$$

Here, $\wp_{\rm ost} = \sqrt{\frac{{\rm d}t}{2\pi}}\exp\left\{-\frac{y_t^2}{2{\rm d}t}\right\}$ is an obtensible probability [7]. From the results above, we can say that this approach works fine for a small time increment ${\rm d}t$ as shown by the completeness relation in Eq. (3.2). The Itô map satisfies the completeness relation and the Lindblad master equation only to the first order in ${\rm d}t$.

For multiple channels with the system's Hamiltonian $\hat{H}$, the measurement operator is given by

$$\hat{M}_{\rm I} \;=\; \hat{1} - \left(i\hat{H} + \tfrac{1}{2}\sum_r \eta_r\hat{L}_r^\dagger\hat{L}_r\right){\rm d}t + \sum_r \sqrt{\eta_r}\hat{L}_r y_t{\rm d}t, \tag{3.4}$$

where $\hat{L}_r$ is the measured channel. The state update is given by

$$\rho(t+{\rm d}t) \;=\; \frac{\hat{M}_{\rm I}\rho(t)\hat{M}_{\rm I}^\dagger + \sum_j \mathcal{D}[\hat{V}_j]\rho(t){\rm d}t + \sum_r \mathcal{D}[\sqrt{1-\eta_r}\hat{L}_r]\rho(t){\rm d}t}{{\rm Tr}\left[\hat{M}_{\rm I}\rho(t)\hat{M}_{\rm I}^\dagger + \sum_j \mathcal{D}[\hat{V}_j]\rho(t){\rm d}t + \sum_r \mathcal{D}[\sqrt{1-\eta_r}\hat{L}_r]\rho(t){\rm d}t\right]}, \tag{3.5}$$

where $\hat{V}_j$ is the unmeasured channel.

3.2 Rouchon-Ralph Approach

In 2015, Rouchon and Ralph [1] proposed the measurement operator to improve the precision in computing quantum trajectories used in quantum feedback control. They began with the idea of the Euler-Milstien scheme which is an extension of the Itô SDE with terms of the second order in the Wiener increment ($\mathrm{d}W^2$) [30]. They implemented such scheme to quantum stochastic master equation [1] and proposed the measurement operator of the form

$$\hat{M}_{\mathrm{R}}(y_t) \;=\; \hat{1} + \big(\hat{c}y_t - \frac{1}{2}\hat{c}^\dagger\hat{c}\big)\mathrm{d}t + \frac{1}{2}\hat{c}^2\big(y_t^2\mathrm{d}t^2 - \mathrm{d}t\big), \tag{3.6}$$

where $\hat{c}$ and y_t are the same Lindblad operator and the measurement record as before. Noting that with the Itô rule, we get $y_t^2\mathrm{d}t^2 \sim \mathrm{d}t$ and we can see that $\hat{M}_{\mathrm{R}} = \hat{M}_{\mathrm{I}}$.

We then again perform the calculation for the completeness relation and the Lindblad master equation as follows.

- Completeness relation:

$$\int \mathrm{d}y_t \wp_{\mathrm{ost}} \hat{M}_{\mathrm{R}}^\dagger(y_t)\hat{M}_{\mathrm{R}}(y_t) \;=\; \hat{1} + \left(\frac{1}{4}(\hat{c}^\dagger\hat{c})^2 + \frac{1}{2}(\hat{c}^\dagger)^2\hat{c}^2\right)\mathrm{d}t^2 + \mathcal{O}(\mathrm{d}t^3) \tag{3.7}$$

- Lindblad master equation:

$$\begin{aligned}\rho(t+\mathrm{d}t) \;&=\; \int \mathrm{d}y_t \wp_{\mathrm{ost}} \hat{M}_{\mathrm{R}}(y_t)\rho(t)\hat{M}_{\mathrm{R}}^\dagger(y_t) \\ &=\; \rho(t) + \mathcal{D}[\hat{c}]\rho(t)\mathrm{d}t + \left(\frac{1}{4}\hat{c}^\dagger\hat{c}\rho(t)\hat{c}^\dagger\hat{c} + \frac{1}{2}\hat{c}^2\rho(t)(\hat{c}^\dagger)^2\right)\mathrm{d}t^2 + \mathcal{O}(\mathrm{d}t^3)\end{aligned} \tag{3.8}$$

We again show that $\hat{M}_{\mathrm{R}}$ satisfies the completeness relation and the Lindblad master equation only to the first order in $\mathrm{d}t$.

In Ref. [1], the map was also generalised to multiple channels with the system's

Hamiltonian $\hat{H}$, which is given by

$$\hat{M}_{\mathrm{R}} = \hat{1} - \left(i\hat{H} + \tfrac{1}{2}\sum_j \hat{V}_j^\dagger \hat{V}_j + \tfrac{1}{2}\sum_r \hat{L}_r^\dagger \hat{L}_r \right) \mathrm{d}t + \sum_r \sqrt{\eta_r}\hat{L}_r y_t \mathrm{d}t + \sum_{r,s} \tfrac{\sqrt{\eta_r \eta_s}}{2} \hat{L}_r \hat{L}_s (y_{t,r} y_{t,s} \mathrm{d}t^2 - \delta_{r,s}\mathrm{d}t), \quad (3.9)$$

where the state update is given by

$$\rho(t+\mathrm{d}t) = \frac{\hat{M}_{\mathrm{R}}\rho(t)\hat{M}_{\mathrm{R}}^\dagger + \sum_j \hat{V}_j \rho(t) \hat{V}_j^\dagger \mathrm{d}t + \sum_r (1-\eta_r)\hat{L}_r \rho(t) \hat{L}_r^\dagger \mathrm{d}t}{\mathrm{Tr}\left[\hat{M}_{\mathrm{R}}\rho(t)\hat{M}_{\mathrm{R}}^\dagger + \sum_j \hat{V}_j \rho(t) \hat{V}_j^\dagger \mathrm{d}t + \sum_r (1-\eta_r)\hat{L}_r \rho(t) \hat{L}_r^\dagger \mathrm{d}t\right]}, \quad (3.10)$$

noting that $\hat{L}_r$ and $\hat{V}_j$ are Lindblad operators for measured and dephasing channels, respectively.

3.3 Guevara-Wiseman Approach

This approach was proposed by Guevara and Wiseman in [2]. They proposed the complete positivity map for quantum trajectories with jumps and diffusive measurements and used it for quantum state smoothing. They started with the idea to improve the completeness relation of the Itô measurement operator in Eq. (3.2) to second order in $\mathrm{d}t$. Therefore, they intuitively proposed the measurement operator

$$\hat{M}_{\mathrm{G}}(y_t) = \hat{1} + \left(y_t \hat{c} - \frac{1}{2}\hat{c}^\dagger \hat{c}\right)\mathrm{d}t - \frac{1}{8}(\hat{c}^\dagger \hat{c})^2 \mathrm{d}t^2, \quad (3.11)$$

by adding the extra term from the Itô map in Eq. (3.1).

We then perform the calculation of the completeness relation and the Lindblad master equation as follows.

- Completeness relation:

$$\int \mathrm{d}y_t \wp_{\mathrm{ost}} \hat{M}_{\mathrm{G}}^\dagger(y_t)\hat{M}_{\mathrm{G}}(y_t) = \hat{1} + \mathcal{O}(\mathrm{d}t^3) \quad (3.12)$$

- Lindblad master equation:

$$\begin{aligned} \rho(t+\mathrm{d}t) &= \int \mathrm{d}y_t \wp_{\mathrm{ost}} \hat{M}_{\mathrm{G}}(y_t)\rho(t)\hat{M}_{\mathrm{G}}^{\dagger}(y_t) \\ &= \rho(t) + \mathcal{D}[\hat{c}]\rho(t)\mathrm{d}t + \frac{1}{4}\mathcal{D}[\hat{c}^{\dagger}\hat{c}]\rho(t)\mathrm{d}t^2 + \mathcal{O}(\mathrm{d}t^3) \end{aligned} \tag{3.13}$$

It is clear that the completeness relation is satisfied to second order in $\mathrm{d}t$. However, the Lindblad master equation is correct only to the first order in $\mathrm{d}t$. It is still not enough for our criterions. Therefore, in the next chapter, we will propose a new measurement operator that can satisfy the completeness relation and the Lindblad master equation both to the order $\mathrm{d}t^2$.

Chapter 4

Constructing High-order Completely Positive Map

We here derive a suitable measurement operator from the basic assumption that a quantum system is interacting with an environment. We consider a primary system described by ρ, coupled to a bosonic bath (which plays the role of the environment). This chapter is organised as follows. We first derive the high-order completely positive map for a simple case, which is the map for a single Lindblad operator, no system's Hamiltonian, and no extra dephasing. In Section 4.2, we derive the map for a more general case, we add the system's Hamiltonain with multiple extra dephasing channels. Finally, we end this chapter with the examples for qubit z-measurement and fluorescence measurement.

4.1 Measurement Operator for One Channel

In all our examples below the primary system is a qubit, but the derivation should apply for any quantum system ρ. Considering the interaction frame and the rotating–wave approximation [7, 14], the coupling unitary operator representing an infinitesimal evolution in Heisenberg picture is given by,

$$\hat{U}(t+\mathrm{d}t,t) = \exp\left[\hat{c}\,\mathrm{d}\hat{B}^{\dagger} - \hat{c}^{\dagger}\mathrm{d}\hat{B}\right], \tag{4.1}$$

Order	Hermite polynomials
$H_0(y)$	1
$H_1(y)$	y
$H_2(y)$	y^2-1
$H_3(y)$	y^3-3y
$H_4(y)$	y^4-6y^2+3

Table 4.1: This table shows the fist four orders of the Hermite polynomials.

which is from the coupling Hamiltonian $\hat{V}_{\mathrm{IF}} = i(\hat{c}\,\mathrm{d}\hat{B}^\dagger - \hat{c}^\dagger \mathrm{d}\hat{B})$, where $\hat{c}$ is the system's Lindblad operator describing the coupling to the bath. $\mathrm{d}\hat{B}$ is an infinitesimal operator for the bath excitation satisfying a commutator relationship $[\mathrm{d}\hat{B}, \mathrm{d}\hat{B}^\dagger] = \mathrm{d}t$.

Assuming that the bath initial state is in a vacuum state $|0\rangle_{\mathrm{b}}$ and, after the interaction with the system via the unitary operator Eq. (4.1), the state is projected onto a homodyne eigenstate $|y_t\rangle$ corresponding to a detector readout y_t, we can derive a measurement operator from

$$ {}_{\mathrm{b}}\langle y_t|\hat{U}_1|0\rangle_{\mathrm{b}} = {}_{\mathrm{b}}\langle y_t| \left(\hat{1} + \hat{c}\,\mathrm{d}\hat{B} - \tfrac{1}{2}\hat{c}^\dagger\hat{c}\,\mathrm{d}\hat{B}\mathrm{d}\hat{B}^\dagger + \tfrac{1}{2}\hat{c}^2(\mathrm{d}\hat{B}^\dagger)^2\right)|0\rangle_{\mathrm{b}}, \tag{4.2}$$

where $\hat{U}_1$ is denoted as the expansion of the unitary operator $\hat{U}(t+\mathrm{d}t, t)$ up to $\mathcal{O}(\mathrm{d}t, \mathrm{d}\hat{B}^2)$, ignoring terms with $\mathrm{d}\hat{B}$ to its right as they give zero when operating on the vacuum state. For the diffusive measurement, it is sufficient to consider a quadrature measurement of the bath state (which is bosonic), where the bath eigenstates are the quadrature states $y_t \in \{I, Q\}$. We use the fact that $\mathrm{d}\hat{B}^\dagger$ creates an excitation in the bath $\mathrm{d}\hat{B}^\dagger|n\rangle_{\mathrm{b}} = \sqrt{(n+1)\mathrm{d}t}|n+1\rangle_{\mathrm{b}}$ with a factor of $\sqrt{\mathrm{d}t}$, and the normalised wavefunctions of a Harmonic oscillator given in terms of Hermite polynomials H_n for the projection of number states (see Table 4.1)

$$ {}_{\mathrm{b}}\langle y_t|n\rangle_{\mathrm{b}} = (1/\sqrt{2^n n!})(\alpha/\pi)^{1/4}\exp\!\left(-\alpha y^2/2\right)H_n(\sqrt{\alpha}\,y_t), \tag{4.3}$$

where $\alpha = \mathrm{d}t/2$. We then obtain the measurement operator, which perfectly agrees

with the Rouchon-Ralph measurement operator in Eq. (3.6), for a generalised homodyne measurement to order of $\mathcal{O}(\mathrm{d}t, \mathrm{d}\hat{B}^2)$ as,

$$\hat{M}_{\mathrm{R}} = \wp(y_t)\left\{\hat{1} - \tfrac{1}{2}\hat{c}^\dagger\hat{c}\,\mathrm{d}t + y_t\hat{c}\,\mathrm{d}t + \tfrac{1}{2}\hat{c}^2(y_t^2\mathrm{d}t^2 - \mathrm{d}t) \quad , \right. \tag{4.4}$$

where $\wp(y_t) = (\mathrm{d}t/2\pi)^{1/4}\exp(-y_t^2\mathrm{d}t/4)$.

As shown in Section 3.2 the Rouchon-Ralph measurement operator does not meet our criterions, especially, the terms from the completeness relation, so that we need to find some extra terms to cancel them. We therefore consider the high-order expansion of the unitary operator $\hat{U}(t+\mathrm{d}t, t)$. We again ignore the expansion terms with $\mathrm{d}\hat{B}$ to its right. Here, we show the first four orders of the argument's expansion. We can start by performing the Taylor expansion of Eq. (4.1) up to $\mathcal{O}(\mathrm{d}t^2, \mathrm{d}\hat{B}^4)$, and defining $\hat{U}(t+\mathrm{d}t, t) \equiv \exp[\hat{\alpha}]$, giving

$$e^{\hat{\alpha}} \approx \hat{1} + \hat{\alpha} + \tfrac{1}{2}\hat{\alpha}^2 + \tfrac{1}{6}\hat{\alpha}^3 + \tfrac{1}{24}\hat{\alpha}^4, \tag{4.5}$$

where we have used $\hat{\alpha} = \hat{c}\mathrm{d}\hat{B}^\dagger - \hat{c}^\dagger\mathrm{d}\hat{B}$. Applying the initial and final states of the bath, we obtain

$$\begin{aligned}
{}_{\mathrm{b}}\langle y_t|\,\hat{\alpha}^0|0\rangle_{\mathrm{b}} &= \hat{1}, \\
{}_{\mathrm{b}}\langle y_t|\,\hat{\alpha}^1|0\rangle_{\mathrm{b}} &= {}_{\mathrm{b}}\langle y_t|\,\hat{c}\mathrm{d}\hat{B}^\dagger|0\rangle_{\mathrm{b}} = y_t\hat{c}\mathrm{d}t, \\
{}_{\mathrm{b}}\langle y_t|\,\hat{\alpha}^2|0\rangle_{\mathrm{b}} &= {}_{\mathrm{b}}\langle y_t|\,\hat{c}^2(\mathrm{d}\hat{B}^\dagger)^2 - \hat{c}^\dagger\hat{c}\mathrm{d}\hat{B}\mathrm{d}\hat{B}^\dagger|0\rangle_{\mathrm{b}} = \left[\hat{c}^2(y_t^2\mathrm{d}t - 1) - \hat{c}^\dagger\hat{c}\right]\mathrm{d}t, \\
{}_{\mathrm{b}}\langle y_t|\,\hat{\alpha}^3|0\rangle_{\mathrm{b}} &= {}_{\mathrm{b}}\langle y_t|\,\hat{c}^3(\mathrm{d}\hat{B}^\dagger)^3 - \hat{c}^\dagger\hat{c}^2\mathrm{d}\hat{B}(\mathrm{d}\hat{B}^\dagger)^2 - \hat{c}\hat{c}^\dagger\hat{c}\mathrm{d}\hat{B}^\dagger\mathrm{d}\hat{B}\mathrm{d}\hat{B}^\dagger|0\rangle_{\mathrm{b}} \\
&= \left[\hat{c}^3(y_t^3\mathrm{d}t - 3y_t) - 2y_t\hat{c}^\dagger\hat{c}^2 - y_t\hat{c}\hat{c}^\dagger\hat{c}\right]\mathrm{d}t^2, \\
{}_{\mathrm{b}}\langle y_t|\,\hat{\alpha}^4|0\rangle_{\mathrm{b}} &= {}_{\mathrm{b}}\langle y_t|\,\hat{c}^4(\mathrm{d}\hat{B}^\dagger)^4 - \hat{c}^\dagger\hat{c}^3\mathrm{d}\hat{B}(\mathrm{d}\hat{B}^\dagger)^3 - \hat{c}\hat{c}^\dagger\hat{c}^2\mathrm{d}\hat{B}^\dagger\mathrm{d}\hat{B}(\mathrm{d}\hat{B}^\dagger)^2 \\
&\quad -\hat{c}^2\hat{c}^\dagger\hat{c}(\mathrm{d}\hat{B}^\dagger)^2\mathrm{d}\hat{B}\mathrm{d}\hat{B}^\dagger + (\hat{c}^\dagger\hat{c})^2(\mathrm{d}\hat{B}\mathrm{d}\hat{B}^\dagger)^2 + (\hat{c}^\dagger)^2\hat{c}^2\mathrm{d}\hat{B}^2(\mathrm{d}\hat{B}^\dagger)^2|0\rangle_{\mathrm{b}} \\
&= \left[\hat{c}^4(y_t^4\mathrm{d}t^2 - 6y_t\mathrm{d}t + 3) - 3\hat{c}^\dagger\hat{c}^3(y_t^2\mathrm{d}t - 1) - 2\hat{c}\hat{c}^\dagger\hat{c}^2(y_t^2\mathrm{d}t - 1)\right. \\
&\quad \left. -3\hat{c}^2\hat{c}^\dagger\hat{c}^3(y_t^2\mathrm{d}t - 1) + (\hat{c}^\dagger\hat{c})^2 + 2(\hat{c}^\dagger)\hat{c}^2\right]\mathrm{d}t^2,
\end{aligned} \tag{4.6}$$

where we have left the ostensible probability $\wp_{\mathrm{ost}} = \sqrt{\frac{\mathrm{d}t}{2\pi}}\exp[-y_t^2\mathrm{d}t/4]$ outside the

calculation.

We remark that in the first three orders of the $\hat{\alpha}$ expansion contribute to the Rouchon-Ralph approach in Eq. (3.6). Here, we can construct the measurement operator by keeping all terms of the expansion. However, when calculating the completeness relation some terms will be vanished by themselves, that is because

$$\int \wp_{\rm ost}(y_t^4 \mathrm{d}t^4 - 3y_t^2 \mathrm{d}t^3)\mathrm{d}y_t = 0, \tag{4.7}$$

$$\int \wp_{\rm ost}(y_t^4 \mathrm{d}t^4 - 6y_t \mathrm{d}t^3 + 3\mathrm{d}t^2)\mathrm{d}y_t = 0, \tag{4.8}$$

$$\int \wp_{\rm ost}(y_t^2 \mathrm{d}t^3 - \mathrm{d}t^2)\mathrm{d}y_t = 0, \tag{4.9}$$

and any terms with higher orders than $\mathcal{O}(\mathrm{d}t^2, \mathrm{d}\hat{B}^4)$ also vanish. Therefore, what left are terms from $\hat{\alpha}^3$: (a) $y_t \hat{c}^\dagger \hat{c}^2 \mathrm{d}t^2$ and (b) $y_t \hat{c}\hat{c}^\dagger \hat{c}\mathrm{d}t^2$, and from $\hat{\alpha}^4$: (c) $(\hat{c}^\dagger \hat{c})^2 \mathrm{d}t^2$ and (d) $(\hat{c}^\dagger)^2 \hat{c}^2 \mathrm{d}t^2$. We can show that the (d) term is not needed when calculating the unconditioned state update. Finally, we select the (a)-(c) terms with the suitable coefficients.

We select the term $1/8(\hat{c}^\dagger \hat{c})^2(\mathrm{d}\hat{B}\mathrm{d}\hat{B}^\dagger)^2$ with coefficient $1/8$, because this coefficient can give back the unconditioned state update agreeing with the Lindblad master equation in Eq. (2.14). The two more terms are $-1/8\hat{c}^\dagger \hat{c}^2 \mathrm{d}\hat{B}(\mathrm{d}\hat{B}^\dagger)^2$ and $-1/4\hat{c}\hat{c}^\dagger \hat{c}\mathrm{d}\hat{B}^\dagger \mathrm{d}\hat{B}\mathrm{d}\hat{B}^\dagger$, where the coefficients are chosen as a result of the first term. Now, we can construct the measurement operator from

$${}_{\rm b}\langle y_t|\hat{U}_2|0\rangle_{\rm b} = {}_{\rm b}\langle y_t|\hat{U}_1 + \tfrac{1}{8}(\hat{c}^\dagger \hat{c})^2(\mathrm{d}\hat{B}\mathrm{d}\hat{B}^\dagger)^2 - \tfrac{1}{8}\hat{c}^\dagger \hat{c}^2 \mathrm{d}\hat{B}(\mathrm{d}\hat{B}^\dagger)^2 - \tfrac{1}{4}\hat{c}\hat{c}^\dagger \hat{c}\mathrm{d}\hat{B}^\dagger \mathrm{d}\hat{B}\mathrm{d}\hat{B}^\dagger|0\rangle_{\rm b}, \tag{4.10}$$

where $\hat{U}_2$ is defined as the part of the unitary operator that has the high-order expansion of $\hat{U}(t+\mathrm{d}t, t)$ up to $\mathcal{O}(\mathrm{d}t^2, \mathrm{d}\hat{B}^4)$. Therefore, the measurement operator is given by

$$\hat{M}_{\rm W}(y_t) = \hat{1} - \tfrac{1}{2}(\hat{c}^2 + \hat{c}^\dagger \hat{c})\mathrm{d}t + \tfrac{1}{8}\big(\hat{c}^\dagger \hat{c}\big)^2 \mathrm{d}t^2 + \big[\hat{c}\mathrm{d}t - \tfrac{1}{4}\big(\hat{c}^\dagger \hat{c}^2 + \hat{c}\hat{c}^\dagger \hat{c}\big)\mathrm{d}t^2\big]y_t + \tfrac{1}{2}\hat{c}^2 \mathrm{d}t^2 y_t^2. \tag{4.11}$$

Approach	Completeness relation	$\mathcal{O}(\mathrm{d}t^2)$ of the state update
$\hat{M}_{\mathrm{I}}$	$1+\mathcal{O}(\mathrm{d}t^2)$	$\frac{1}{4}\hat{c}^\dagger\hat{c}\rho(t)\hat{c}^\dagger\hat{c}$
$\hat{M}_{\mathrm{R}}$	$1+\mathcal{O}(\mathrm{d}t^2)$	$\frac{1}{4}\hat{c}^\dagger\hat{c}\rho(t)\hat{c}^\dagger\hat{c}+\frac{1}{2}\hat{c}^2\rho(t)(\hat{c}^\dagger)^2$
$\hat{M}_{\mathrm{G}}$	$1+\mathcal{O}(\mathrm{d}t^3)$	$\frac{1}{4}\mathcal{D}[\hat{c}^\dagger\hat{c}]\rho(t)$
$\hat{M}_{\mathrm{W}}$	$1+\mathcal{O}(\mathrm{d}t^3)$	$\frac{1}{2}\mathcal{D}[\hat{c}]\big[\mathcal{D}[\hat{c}]\rho(t)\big]$

Table 4.2: We show the comparison among 4 different approaches with our criterions (completeness relation and agreement with the Lindblad master equation) in the scenario of the system's Hamiltonian $\hat{H}=0$ and a single Lindblad operator $\hat{c}$. Noting that we show merely the second order in $\mathrm{d}t$ of the unconditioned system evolution since all approaches are correct to the first order in $\mathrm{d}t$ comparing with the unconditioned Lindblad master equation.

Noting that the new map yields three extra terms of $\hat{M}_{\mathrm{R}}$ which are the forms after projecting onto the bath eigenstate with $\hat{U}_2(t+\mathrm{d}t,t)$.

We perform the calculation of the completeness relation and the unconditioned state update as follows.

- Completeness relation:

$$\int \mathrm{d}y_t \wp_{\mathrm{ost}} \hat{M}_{\mathrm{W}}^\dagger(y_t)\hat{M}_{\mathrm{W}}(y_t) \;=\; \hat{1}+\mathcal{O}(\mathrm{d}t^3) \tag{4.12}$$

- Lindblad master equation:

$$\begin{aligned}\rho(t+\mathrm{d}t) &= \int \mathrm{d}y_t \wp_{\mathrm{ost}} \hat{M}_{\mathrm{W}}(y_t)\rho(t)\hat{M}_{\mathrm{W}}^\dagger(y_t) \\ &= \rho(t)+\mathcal{D}[\hat{c}]\rho(t)\mathrm{d}t+\tfrac{1}{2}\mathcal{D}[\hat{c}]\big[\mathcal{D}[\hat{c}]\rho(t)\big]\mathrm{d}t^2+\mathcal{O}(\mathrm{d}t^3)\end{aligned} \tag{4.13}$$

It is obvious that this measurement operator perfectly satisfies our criterions. The map satisfies the completeness relation to second order in $\mathrm{d}t$ and agree with the Lindblad master equation Eq. (2.14) to second order in $\mathrm{d}t$. We show the comparison among four different approaches in Table 4.2.

4.2 Measurement Operator for Multiple Channels with the System's Hamiltonian

So far, we have derived the measurement operator for one channel without the system's Hamiltonian. To generalise such the measurement operator, we add the system's Hamiltonian $\hat{H}$ to the unitary evolution, giving

$$\hat{U}_{\hat{H}}(t+\mathrm{d}t,t) = \exp\left[-i\hat{H}\mathrm{d}t + \hat{c}\,\mathrm{d}\hat{B}^\dagger - \hat{c}^\dagger \mathrm{d}\hat{B}\right]. \tag{4.14}$$

We can derive the high-order completely positive measurement operator with the unitary evolution in the similar way as we have done in the previous section. Let us consider $\hat{U}_{\hat{H}}(t+\mathrm{d}t,t)$ in Eq. (4.14), we can expand the arguments and keep suitable forms to meet our criterions as

$$\begin{aligned} {}_{\mathrm{b}}\langle y_t|\hat{U}_{\hat{H}_2}|0\rangle_{\mathrm{b}} = {}& {}_{\mathrm{b}}\langle y_t|\,\hat{U}_2 - i\hat{H}\mathrm{d}t - \tfrac{1}{2}\hat{H}^2\mathrm{d}t^2 - \tfrac{i}{2}\mathrm{d}t(\hat{H}\hat{c}+\hat{c}\hat{H})\mathrm{d}\hat{B}^\dagger \\ & + \tfrac{i}{4}\mathrm{d}t(\hat{c}^\dagger\hat{c}\hat{H}+\hat{H}\hat{c}^\dagger\hat{c})\mathrm{d}\hat{B}\mathrm{d}\hat{B}^\dagger|0\rangle_{\mathrm{b}}, \end{aligned} \tag{4.15}$$

where $\hat{U}_{\hat{H}_2}$ denotes the selected suitable forms of the unitary evolution expansion up to $\mathcal{O}(\mathrm{d}t^2, \mathrm{d}\hat{B}^4)$. We then obtain the full evolution of the measurement operator for a single perfectly measured channel,

$$\begin{aligned} \hat{M}^*_{\mathrm{W}}(y_t) = \hat{1} - i\hat{H}\mathrm{d}t - \tfrac{1}{2}(\hat{c}^2+\hat{c}^\dagger\hat{c})\mathrm{d}t + \left[\tfrac{1}{8}\left(\hat{c}^\dagger\hat{c}\right)^2 + \tfrac{i}{4}\left(\hat{c}^\dagger\hat{c}\hat{H}+\hat{H}\hat{c}^\dagger\hat{c}\right) - \tfrac{1}{2}\hat{H}^2\right]\mathrm{d}t^2 \\ + \left(\hat{c}\mathrm{d}t - \left[\tfrac{1}{4}\left(\hat{c}^\dagger\hat{c}^2+\hat{c}\hat{c}^\dagger\hat{c}\right) + \tfrac{i}{2}\left(\hat{c}\hat{H}+\hat{H}\hat{c}\right)\right]\mathrm{d}t^2\right)y_t + \tfrac{1}{2}\hat{c}^2\mathrm{d}t^2 y_t^2. \end{aligned} \tag{4.16}$$

Here, we can see that the unitary parts will finally become terms from $\mathcal{L}_0 + \mathcal{L}_0^2$ itself and from the crossed term with the decoherence operator $\hat{c}$ as $\mathcal{L}_0[\mathcal{D}] + \mathcal{D}[\mathcal{L}_0]$.

Let us consider the measurement operator with multiple channels. We can define a set of decoherence operators with $N = 2n + m$ operators. The set includes n operators for measured channels i.e., $\hat{L}_\nu \in \{\sqrt{\eta_1}\hat{c}_1, ..., \sqrt{\eta_n}\hat{c}_n\}$, $m+n$ operators for unmeasured channels i.e., $\hat{V}_{\tilde{\nu}} \in \{\hat{V}_1, ..., \hat{V}_m, \sqrt{1-\eta_1}\hat{c}_1, ..., \sqrt{1-\eta_n}\hat{c}_n\}$, η_r is the mea-

surement efficiencies. Here, the generalised measurement operator can be written as $\hat{M} = \sum_{k\neq j}^{N} \hat{M}(\hat{V}_k)\hat{M}(\hat{V}_j)$, giving

$$\begin{aligned}\hat{M}^{\star}_{\mathrm{W}}(y_t) =& \hat{1} + \sum_{k\in\mu}\Big(-\tfrac{1}{2}\hat{V}_k^{\dagger}\hat{V}_k \mathrm{d}t + y_k\hat{V}_k\mathrm{d}t + \tfrac{1}{2}\hat{V}_k^2[y_k^2\mathrm{d}t^2 - \mathrm{d}t] + \tfrac{1}{8}\big(\hat{V}_k^{\dagger}\hat{V}_k\big)^2\mathrm{d}t^2 \\ &- \tfrac{1}{4}y_k\big[\hat{V}_k^{\dagger}\hat{V}_k^2 + \hat{V}_k\hat{V}_k^{\dagger}\hat{V}_k\big]\mathrm{d}t^2 + \tfrac{i}{4}\{\hat{V}_k^{\dagger}\hat{V}_k, \hat{H}\}\mathrm{d}t^2 - \tfrac{i}{2}y_k\{\hat{V}_k, \hat{H}\}\mathrm{d}t^2\Big) \\ &+ \sum_{j\neq k\in\mu}\left(\tfrac{1}{8}\hat{V}_j^{\dagger}\hat{V}_j\hat{V}_k^{\dagger}\hat{V}_k - \tfrac{1}{4}\hat{V}_j^{\dagger}\hat{V}_j\hat{V}_k y_k - \tfrac{1}{4}\hat{V}_j\hat{V}_k^{\dagger}\hat{V}_k y_j + \tfrac{1}{\sqrt{2}}\hat{V}_j\hat{V}_k y_j y_k\right)\mathrm{d}t^2 \\ &- i\hat{H}\mathrm{d}t - \tfrac{1}{2}\hat{H}^2\mathrm{d}t^2, \end{aligned} \tag{4.17}$$

where $y_{k,j}$ is the measurement readout for the channel k, j. For unmeasured channels, one cannot obtain the measurement readout $y_{\tilde{\nu}}$, we therefore integrate over possible readout, which gives back an average evolution.

In this thesis, we consider a single imperfectly measured channel (i.e., one measured channel $\hat{L}$ and the set of decoherence operators becomes $\{\sqrt{\eta}\hat{L}, \tilde{\nu}\}$). Finally, the full dynamics measurement operator is given by,

$$\begin{aligned}\hat{M}^{\star}_{\mathrm{W}}(y_t) =& \hat{1} - i\hat{H}\mathrm{d}t - \tfrac{\eta}{2}\hat{L}^{\dagger}\hat{L}\mathrm{d}t + \sqrt{\eta}\,y_t\,\hat{L}\mathrm{d}t + \tfrac{\eta}{2}\hat{L}^2[y_t^2\mathrm{d}t^2 - \mathrm{d}t] - \tfrac{1}{2}\hat{H}^2\mathrm{d}t^2 + \tfrac{i}{4}\eta\{\hat{L}^{\dagger}\hat{L}, \hat{H}\}\mathrm{d}t^2 \\ &- \tfrac{i}{2}y_t\sqrt{\eta}\{\hat{L}, \hat{H}\}\mathrm{d}t^2 + \tfrac{1}{8}\eta^2\big(\hat{L}^{\dagger}\hat{L}\big)^2\mathrm{d}t^2 - \tfrac{1}{4}\eta^{3/2}\,y_t\,\big[\hat{L}^{\dagger}\hat{L}^2 + \hat{L}\hat{L}^{\dagger}\hat{L}\big]\mathrm{d}t^2 \\ &- y_t\sum_{j\in\tilde{\nu}}\left(\tfrac{\sqrt{\eta}}{4}\big[\hat{V}_j^{\dagger}\hat{V}_j\hat{L} + \hat{L}\hat{V}_j^{\dagger}\hat{V}_j\big]\mathrm{d}t^2 - \delta\sqrt{\tfrac{\eta}{2}}\big[\hat{V}_j\hat{L} + \hat{L}\hat{V}_j\big]\mathrm{d}t^{3/2}\right), \end{aligned} \tag{4.18}$$

where we have set $\hat{c} = \sqrt{\eta}\hat{L}$ for the measurement channel with the efficiency η. We define δ as $\delta = 0$ except $\delta^2 = 1$. The system state update can be described by

$$\rho(t + \mathrm{d}t) = \frac{\hat{M}^{\star}_{\mathrm{W}}(y_t)\rho(t)\hat{M}^{\star}_{\mathrm{W}}(y_t)^{\dagger} + \mathscr{D}[\hat{V}_j]\rho(t)}{\mathrm{Tr}\Big\{\hat{M}^{\star}_{\mathrm{W}}(y_t)\rho(t)\hat{M}^{\star}_{\mathrm{W}}(y_t)^{\dagger} + \mathscr{D}[\hat{V}_j]\rho(t)\Big\}}, \tag{4.19}$$

where $\mathscr{D}[\{\hat{V}_j\}]\bullet$ is defined as

$$\begin{aligned}\mathscr{D}[\{\hat{V}_j\}]\bullet =&\Bigg(\sum_{j\in\tilde{\nu}}\mathcal{D}_j\bullet\,\mathrm{d}t+\tfrac{1}{2}\Bigg\{\sum_{j\in\tilde{\nu}}\left[\mathcal{L}_0\big(\mathcal{D}_j\bullet\big)+\mathcal{D}_j\big(\mathcal{L}_0\bullet\big)+\mathcal{D}_j\big(\mathcal{D}_j\bullet\big)\right]\\&+\tfrac{1}{4}\sum_{k\neq j}^{N}(\hat{V}_k^\dagger\hat{V}_k\hat{V}_j^\dagger\hat{V}_j,\bullet)-\tfrac{1}{2}\sum_{\substack{k=1\\k\neq j}}^{N}\sum_{j\in\tilde{\nu}}\left[(\hat{V}_k^\dagger\hat{V}_k\hat{V}_j,\bullet\hat{V}_j^\dagger)+(\hat{V}_j\hat{V}_k^\dagger\hat{V}_k,\bullet\hat{V}_j^\dagger)\right]\\&+\tfrac{1}{2}\sum_{k\neq j}^{N}(\hat{V}_k^\dagger\hat{V}_k,\bullet\hat{V}_j^\dagger\hat{V}_j)+\sum_{\substack{k,j\in\tilde{\nu}\\k\neq j}}(\hat{V}_k\hat{V}_j,\bullet\hat{V}_j^\dagger\hat{V}_k^\dagger)\Bigg\}\mathrm{d}t^2\Bigg).\end{aligned}\tag{4.20}$$

Here $\mathcal{L}_0$ is the unitary part of the Lindblad, $\mathcal{L}_0[\bullet]=-i[\hat{H},\bullet]$. We have defined the decoherence channel $\mathcal{D}_i\equiv\mathcal{D}[\hat{V}_i]$, and $(\hat{A},\hat{B})=\hat{A}\hat{B}+\hat{B}^\dagger\hat{A}^\dagger$.

By construction, this generalised measurement operator satisfies the completeness relation to $\mathcal{O}(\mathrm{d}t^2)$ and remains the agreement to the unconditioned state update (via integrating over all measurement readouts y_t) comparing to the Lindblad master equation (with $\hat{H}$) to $\mathcal{O}(\mathrm{d}t^2)$ derived by Steinbach *et al.* in Ref. [16].

4.3 Examples

This section we will apply the high-order completely positive map Eq. (4.16) to two examples of the qubit measurement. One is for the Hermitian z-measurement and another is for a measurement of a qubit's fluorescence.

4.3.1 Qubit z-measurement

Let us consider a qubit continuously measured by a detector that is coupled to the qubit via $\hat{\sigma}_z$ observable. This idea has been studied first time via quantum dots experiments [3–6, 31, 32], where a single electron can be in one of the double quantum dots (dot a and b). The current signal from a nearby quantum point contact is continuously detected depending on whether the location of the electron is in dot a or b. The Hamiltonian evolution of this qubit is $\hat{H}=\frac{\epsilon}{2}\hat{\sigma}_z-\frac{\Delta}{2}\hat{\sigma}_x$ where ϵ is an energy asymmetry between two dot and Δ is a tunnelling rate between two dots. The

Lindblad operator for this case is $\hat{c} \propto \hat{\sigma}_z$. We can construct the high-order completely positive measurement operator as (for perfect measurement, i.e., $\eta = 1$)

$$\hat{M}_{y_t} = \hat{1} - \Gamma\hat{1}\mathrm{d}t + \tfrac{\Gamma^2}{8}\hat{1}\mathrm{d}t^2 + \tfrac{\Gamma}{2}\hat{1}\mathrm{d}t^2 y_t^2 + \left[\Gamma^{1/2}\hat{\sigma}_z\mathrm{d}t - \tfrac{1}{4}\Gamma^{3/2}\big(2\hat{\sigma}_z\big)\mathrm{d}t^2\right]y_t \\ - i\hat{H}\mathrm{d}t + \tfrac{1}{2}\left[i\Gamma\hat{H} - \hat{H}^2 + i\Gamma^{1/2}(\hat{\sigma}_z\hat{H} + \hat{H}\hat{\sigma}_z)y_t\right]\mathrm{d}t^2, \quad (4.21)$$

where $\Gamma = 1/4\tau$, τ is the characteristic measurement time, and y_t is the diffusive measurement readout. Noting that this measurement operator agrees with the expansion of the quantum Bayesian approach [3–5] to $\mathcal{O}(\mathrm{d}t^2)$ defined as

$$\hat{M}_z \;=\; \left(\frac{\mathrm{d}t}{2\pi\tau}\right)^{1/4} \exp\left[-\frac{\mathrm{d}t(\sqrt{\tau}y_t - \hat{\sigma}_z)^2}{4\tau}\right], \quad (4.22)$$

where the unitary evolution can be included by applying $\hat{U} = e^{-i\hat{H}\mathrm{d}t}$ separately (see more in Appendix B).

However, one can ask whether there will be errors coming from non-commuting operation in the quantum Bayesian approach, since this measurement operator itself does not include the unitary evolution part, and both operations do not commute. It justifies that this particular example can be simplified by using our measurement operator.

4.3.2 Measurement of qubit's fluorescence

Quantum fluorescence, especially for a qubit system, examines the energy relaxation or the transition of a quantum state. A transition from high energy levels to lower energy levels will result in an emission of photons at their transition modes. Let us consider a qubit system, which has two states, the ground state $|\mathrm{g}\rangle$, and the excited state $|\mathrm{e}\rangle$. The transition of a qubit from the exited state to the ground state will yield a single photon emission. Therefore, the measurement readout could be discrete numbers, or random real numbers, depending on the detection of photons. The fluorescence measurement can be done by a heterodyne measurement of two quadratures of the fluorescence mode, which results in a diffusive continuous measurement

record [7, 8, 14, 22].

The transition of a qubit state can be described by a Lindblad operator proportional to the lowering operator $\hat{c} \propto \hat{\sigma}_- = |\mathrm{g}\rangle \langle \mathrm{e}|$. We therefore construct the high-order completely positive measurement operator as,

$$\hat{M}_{y_t} = \hat{1} - i\hat{H}\mathrm{d}t - \tfrac{\gamma}{2}(\hat{\sigma}_-^2 + \hat{\sigma}_+\hat{\sigma}_-)\mathrm{d}t + \tfrac{\gamma^2}{8}\big(\hat{\sigma}_+\hat{\sigma}_-\big)^2\mathrm{d}t^2 + \tfrac{\gamma}{2}\hat{\sigma}_-^2\mathrm{d}t^2 y_t^2 - \tfrac{i\gamma^{1/2}}{2}(\hat{\sigma}_-\hat{H} + \hat{H}\hat{\sigma}_-)y_t\mathrm{d}t^2 + \big[\tfrac{i\gamma}{4}(\hat{\sigma}_+\hat{\sigma}_-, \hat{H}) - \tfrac{1}{2}\hat{H}^2\big]\mathrm{d}t^2 + \big[\gamma^{1/2}\hat{\sigma}_-\mathrm{d}t - \tfrac{1}{4}\gamma^{3/2}\big(\hat{\sigma}_+\hat{\sigma}_-^2 + \hat{\sigma}_-\hat{\sigma}_+\hat{\sigma}_-\big)\mathrm{d}t^2\big]y_t, \quad (4.23)$$

where γ is a coupling rate. The rising operator is defined as $\hat{\sigma}_+ = \hat{\sigma}_-^\dagger = |\mathrm{e}\rangle \langle \mathrm{g}|$. y_t is the measurement readout for diffusive quantum fluorescence measurements.

Chapter 5

Numerical Simulations for qubit trajectories

In this section, we aim to make comparison among the approaches introduced in Chapters 3 and 4 by comparing trajectories numerically generated with fine and coarse time resolutions, and checking their agreement with the Lindblad average evolution. We consider the superconducting qubit experiment [20], where the qubit is measured in z basis, as a model for our simulation. We use the values of parameters extracted from the experiment, including the time resolution $\mathrm{d}t = 0.016$ μs, and analyse errors that can occur from different approaches mentioned above. We begin the chapter by introducing the qubit example and its relevant experiment. We then shows numerical results. The results we show in this section are going to be published in Ref. [33].

5.1 Superconducting Qubit z-measurement

We follow the experimental detail as in Ref. [20], which is a continuous measurement of $\hat{\sigma}_z$ observable using the homodyne detection. The experiment consists of the Transmon qubit circuit dispersively coupled to the microwave beams as in Figure 5-1-a. The state of the input microwave beam can be represented by the phase space in Figure 5-1-b. The beam interacts with the qubit and then is amplified by the LJPA. If the state is $|0\rangle$ (or $|1\rangle$) (Figure 5-1-c), the I-quadrature of the beam will get shifted

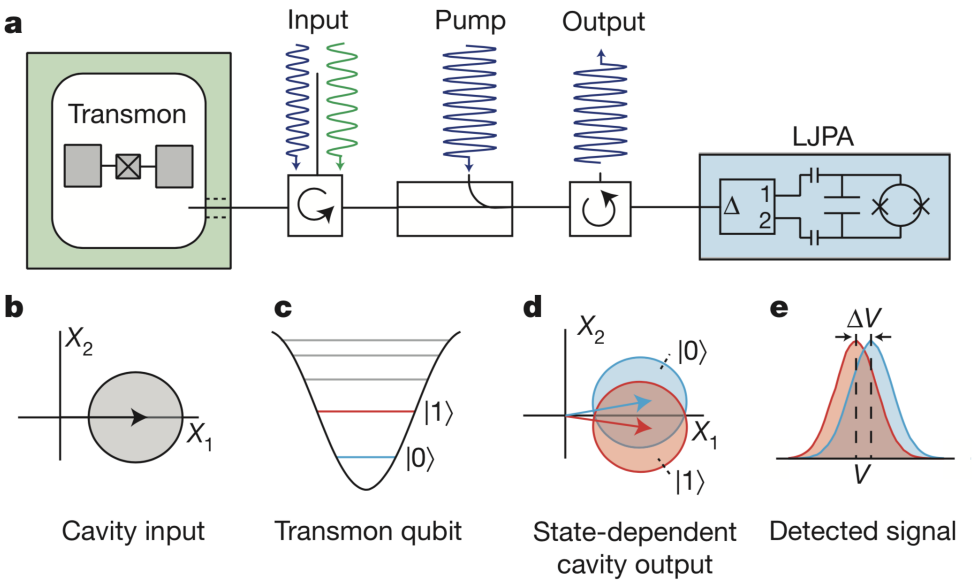

Figure 5-1: This figure displays a brief description of the superconducting qubit experiment. [20]

down (or up) (Figure 5-1-d). Finally, with the homodyne measurement (applied by LJPA) we can transform the detected signal (Figure 5-1-e) to a measurement record and then calculate the quantum trajectories for the transmon qubit. The qubit trajectories for z-measurement was discussed in Section 4.3.1. Here, we will implement four approaches presented in Chapters 3 and 4, using $\hat{M}_{\mathrm{I}}(y_t)$ in Eq. (3.4), $\hat{M}_{\mathrm{R}}(y_t)$ in Eq. (3.9), $\hat{M}^{\star}_{\mathrm{W}}(y_t)$ in Eq. (4.18), and $\hat{M}_{\mathrm{B}}(y_t)$ in Eq. (4.22).

5.2 Simulations

We implement the four approaches for qubit trajectories under the continuous z-measurement. in this thesis, we consider the driven qubit with the Hamiltonian $\hat{H} = \Omega/2\hat{\sigma}_y$, where Ω is the Rabi frequency. The Lindblad operators are $\hat{L} = 1/\sqrt{4\eta\tau}\hat{\sigma}_z$ and $\hat{V} = \sqrt{(1-\eta)/(4\eta\tau)}\hat{\sigma}_z$, describing the measured and unmeasured channels from an imperfect measurement, respectively. We initialise the qubit state $\rho(t_0)$ as $z \equiv \mathrm{Tr}[\rho\hat{\sigma}_z]$ and $x \equiv \mathrm{Tr}[\rho\hat{\sigma}_x]$, where x and z are the Bloch sphere coordinates. Therefore, the Itô

SME Eq. (2.24) gives

$$x(t+\mathrm{d}t) = x(t) - \Gamma x(t)\,\mathrm{d}t + \Omega\, z(t)\,\mathrm{d}t - x(t)\,z(t)\,\big(y(t)-z(t)\big)\mathrm{d}t/\tau, \quad (5.1)$$

$$z(t+\mathrm{d}t) = z(t) - \Omega\, x(t)\,\mathrm{d}t + (1-z(t)^2)\big(y(t)-z(t)\big)\mathrm{d}t/\tau, \quad (5.2)$$

where $\Gamma = \frac{1}{4\eta\tau}$. Noting that there is no y dynamics, since we only consider z-measurement and the qubit rotates about the y-axis in the x-z plane. Here, the measurement record is given by

$$y(t)\mathrm{d}t = \frac{1}{\sqrt{\tau}} z(t)\mathrm{d}t + \mathrm{d}W(t). \quad (5.3)$$

Averaging the Itô SME will result in the last terms in of Eqs. (5.1)-(5.2) vanished, giving back the usual Lindblad evolution. We can solve for the average solution as,

$$z(t) = -\frac{2x_0\Omega}{\beta} e^{-\frac{1}{2}\Gamma t} \sin\left(\frac{\beta t}{2}\right) \quad (5.4)$$

$$x(t) = \frac{x_0}{\beta} e^{-\frac{1}{2}\Gamma t}\left[\beta\cos\left(\frac{\beta t}{2}\right) - \Gamma\sin\left(\frac{\beta t}{2}\right)\right], \quad (5.5)$$

where $\beta \geq 0 = \sqrt{4\Omega^2 - \Gamma^2}$.

In this thesis, we aim to make a comparison among all approaches. Therefore, for a fair comparison, we need to define *true* quantum trajectories as our benchmark. Such trajectories can be generated using a very small time step $\mathrm{d}t$ (in this thesis, we use $\mathrm{d}t = 4\times10^{-4}$ μs), for which, all approaches give the same results. We generate true trajectories using the Itô approach as in Eq. (2.24), where the Wiener increment $\mathrm{d}W(t)$ are generated independently with zero mean and $\langle \mathrm{d}W^2\rangle = \mathrm{d}t$. We can then construct measurement records using Eq. (5.3).

However, in real measurements, too small time step is not possible and it could violate the Markov assumption. In the superconducting transmon qubit experiment, the measurement time step was 0.016 μs [17, 20] . Therefore, we will use $\mathrm{d}t$, which is $\mathrm{d}t = 0.016$ μs for our analysis. We then implement the coarse graining method to rescale the true measurement records from the time step $\mathrm{d}t = 4\times10^{-4}$ μs to

$\mathrm{d}t = 0.016$ μs, using

$$y_{\mathrm{cg}}(\Delta t) \quad = \quad \frac{\mathrm{d}t}{\Delta t} \sum_{t'=\Delta t - \mathrm{d}t}^{\Delta t} y(t'), \tag{5.6}$$

where y_{cg} is the coarse-grained record. in this thesis, the comparison will be done via the trace distance, comparing the trajectories generated from the four approaches with true trajectories and the Lindblad evolution. For a qubit system, the trace distance is defined by [10],

$$D(\rho_{\mathrm{a}}, \rho_{\mathrm{b}}) \quad = \quad \frac{1}{2}|\vec{r}_{\mathrm{a}} - \vec{r}_{\mathrm{b}}|, \tag{5.7}$$

where $\vec{r}_{\mathrm{a}}$ and $\vec{r}_{\mathrm{b}}$ are vectors on the Bloch sphere for the qubit state ρ_{a} and ρ_{b}, respectively. The density matrix of a qubit is written as $\rho = 1/2(\hat{1} + \vec{r} \cdot \vec{\hat{\sigma}})$, where $\vec{\hat{\sigma}}$ are a vector of Pauli matrices defined as $\vec{\hat{\sigma}} = (\hat{\sigma}_x, \hat{\sigma}_y, \hat{\sigma}_z)$ and $\vec{r} = (x, y, z)$.

5.3 Results and Discussions

The qubit trajectories are simulated from $t_0 = 0$ to $T_{\mathrm{f}} = 1.44$ μs, where the initial state is $\rho(t_0) = \frac{1}{2}(\hat{1} + \hat{\sigma}_x)$, i.e., $\vec{r}_0 = (x_0, y_0, z_0) = (1, 0, 0)$.

5.3.1 True Trajectory and Measurement Record Simulation

We first generate $N = 1.5 \times 10^4$ realisations of the Wiener increments with 3,600 time steps using $\mathrm{d}t = 4 \times 10^{-4}$ μs, which are then used to simulate N true qubit trajectories. We check the average of the true trajectories and find that the trace distance comparing with the numerical Lindblad evolution is in order of $\mathcal{O}(10^{-3})$ as shown in Figure 5-2. The true measurement records are then constructed via Eq. (5.3).

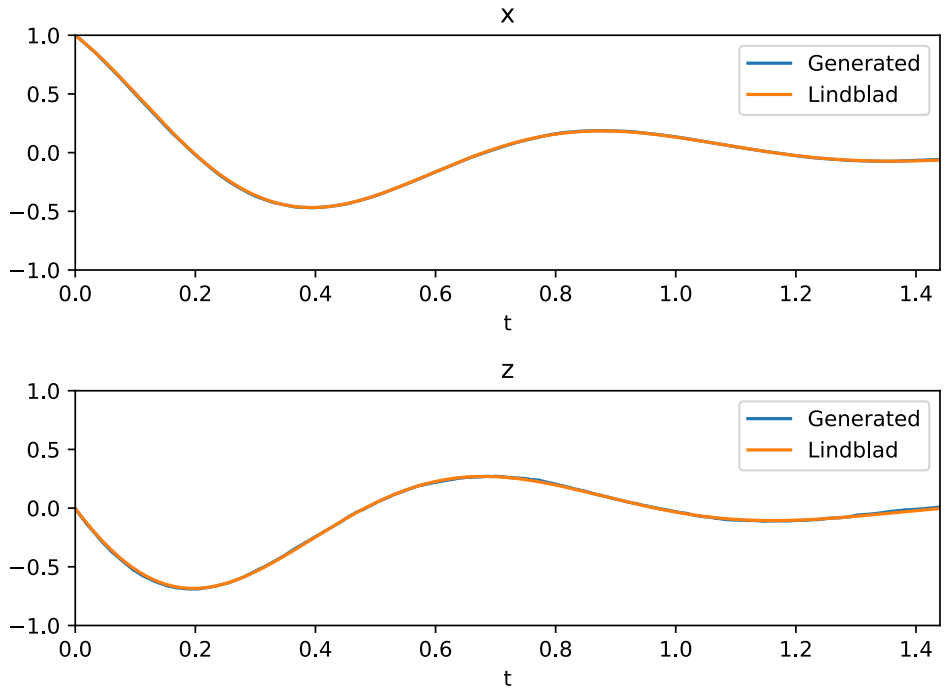

Figure 5-2: This figure displays the averaged generated quantum trajectories comparing with the numerical Lindblad evolution. The parameters are $\Omega/2\pi = 1.08$ MHz, $\tau = 0.315271$ μs, and $\eta = 0.411932$

5.3.2 Coarse Graining Measurement Records for Quantum Trajectories

In this step, we implement the coarse graining method to rescale the true measurement records from Section 5.3.1. This method will change them from 3,600 time steps to 90 time steps per trajectory, corresponding to changing the size of the time step from dt to dt. We then implement the four approaches, using the maps $\hat{M}_{\mathrm{I}}, \hat{M}_{\mathrm{R}}, \hat{M}^{\star}_{\mathrm{W}}$ and $\hat{M}_{\mathrm{B}}$, to process quantum trajectories, for all N trajectories, each having 91 time steps (with the initial point x_0, z_0).

5.3.3 Trace Distance for Individual Trajectories

We then analyse the generated trajectories by calculating the trace distance from the true trajectories with the relevant 90 time steps. The individual trajectories are shown in Figure 5-3. The qubit evolution is stochastic throughout its entire time of

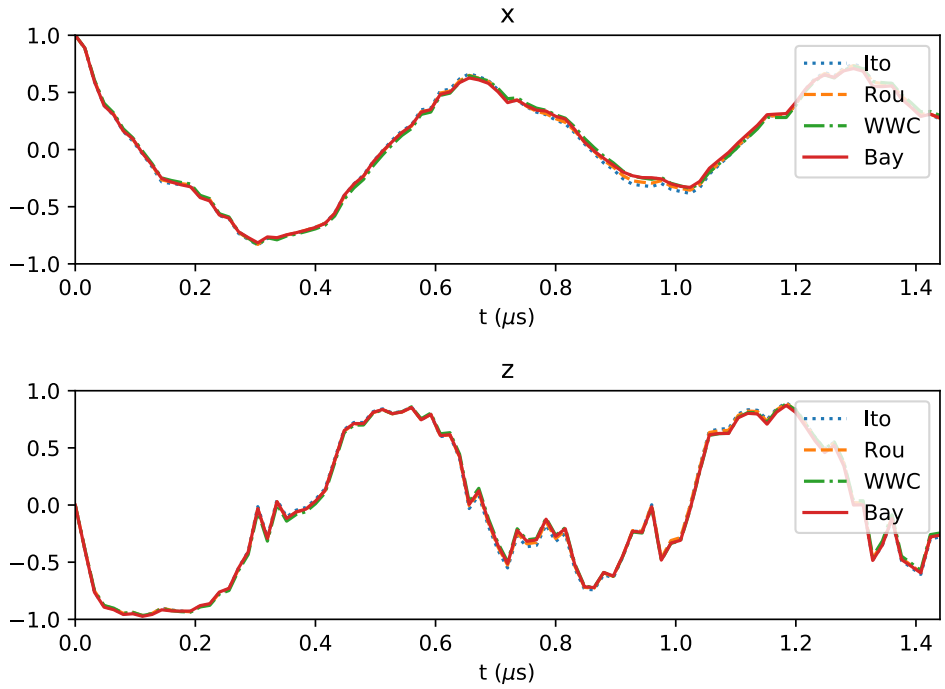

Figure 5-3: The comparison of individual trajectories calculated from the quantum Bayesian (Bay), the Euler-Milstein (Rou), the high-order completely positive map (WWC), and the Itô map (Ito) using the coarse-grained measurement records. Each record has 91 time steps with $\Delta t = 0.016$ μs.

interest and all approaches yield the similar trend, though not exactly the same. We also show the distribution of the trace distance from individual trajectories over N relevant realisations for all four approaches in Figure 5-4, with the average values of the trace distance. The means of the histograms are $\bar{D} = 0.017, 0.013, 0.010$, and 0.019, for $\hat{M}_{\mathrm{I}}, \hat{M}_{\mathrm{R}}, \hat{M}^{\star}_{\mathrm{W}}$ and $\hat{M}_{\mathrm{B}}$, respectively.

5.3.4 Trace Distance for Averaged Trajectories

Finally, we calculate the average trajectories from the N individual trajectories. As shown in Figure 5-6, it is clear that x and z decay to zero as time evolves longer and all approaches give the averages close to the Lindblad solution. We calculate the trace distance of the averaged trajectory from the four approaches comparing with the numerical Lindblad evolution (Eq. (5.4)). The calculations yield the average distances 0.008, 0.005, 0.002, and 0.004, for $\hat{M}_{\mathrm{I}}, \hat{M}_{\mathrm{R}}, \hat{M}^{\star}_{\mathrm{W}}$ and $\hat{M}_{\mathrm{B}}$, respectively. We also show

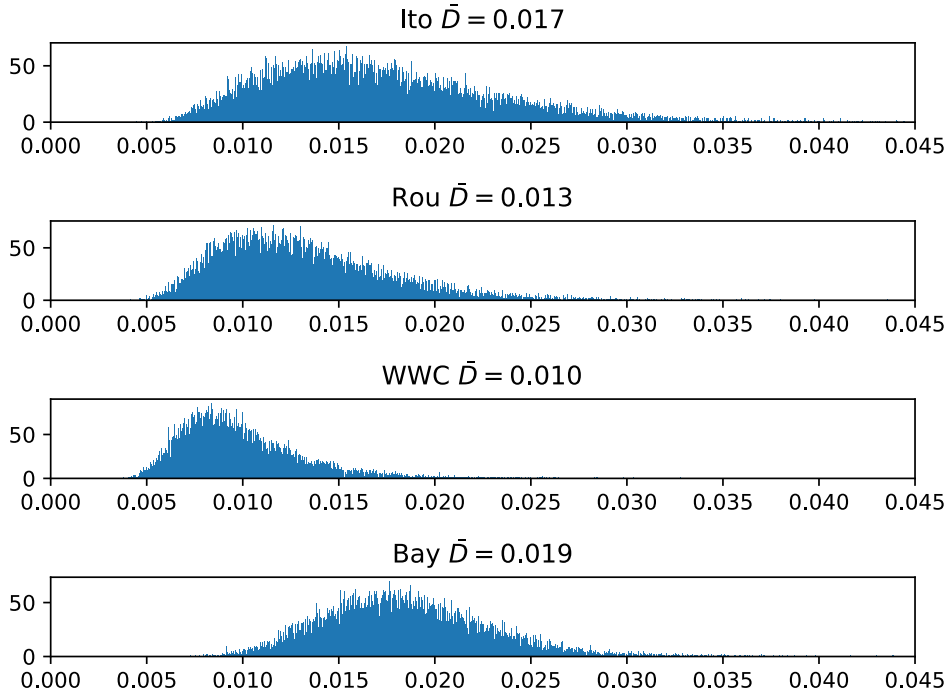

Figure 5-4: This figure displays the distribution of the trace distance comparing with the true trajectories for all approaches.

the trace distance of averaged trajectories changing in time in Figure 5-6. This is clear that the high-order completely positive map is the most accurate method, and the Itô approach is the least accurate one.

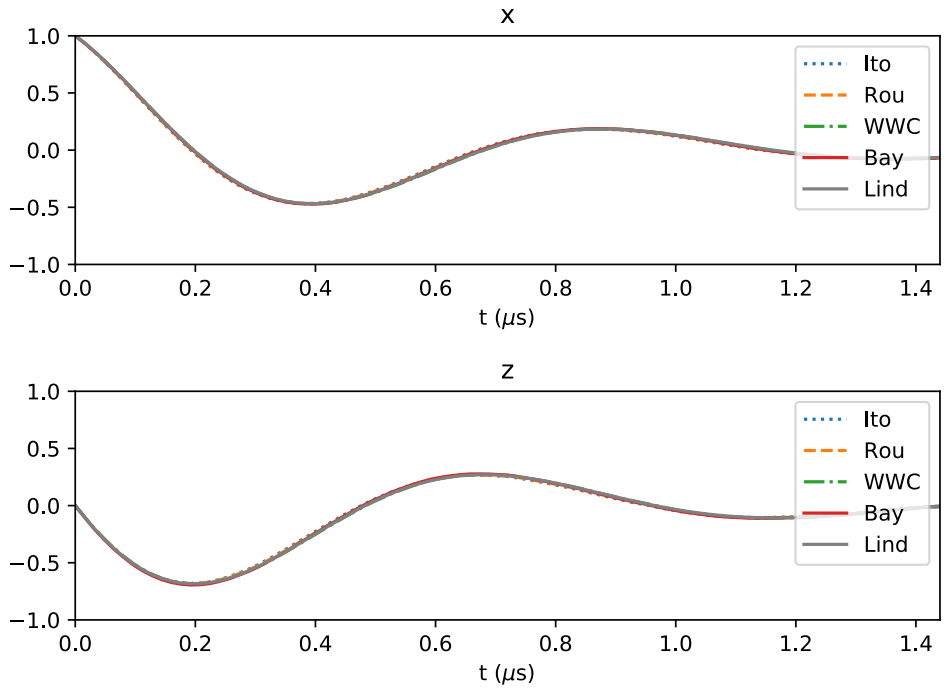

Figure 5-5: This figure displays the plot of averaged trajectory of each approach from $N = 1.5 \times 10^4$ individual trajectories.

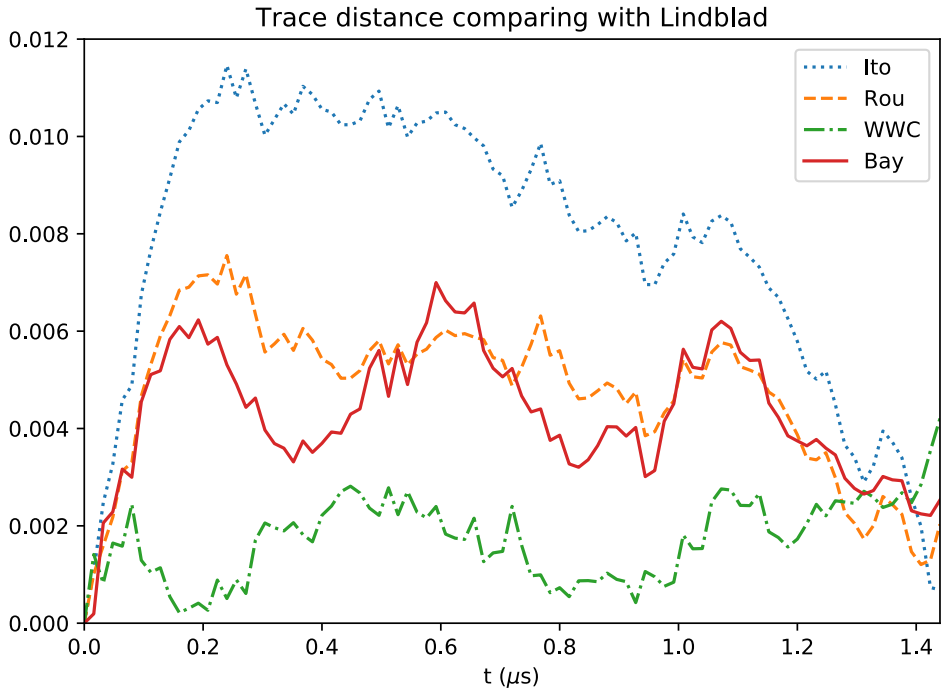

Figure 5-6: This figure displays the changes in time of the trace distance between the averaged trajectory and the numerical Lindblad evolution.

Chapter 6

Conclusion

In this thesis, we discussed about the open quantum system and the continuous quantum measurement, where the unconditioned evolution and the conditioned evolution (quantum trajectory) were obtained. We investigated the concerned problem about the time resolution dt of the measurement operator (map), especially, the error from the completeness relation and the comparison to the Lindblad master equation. The finite time scale can lead to errors in quantum trajectory simulations. We reviewed the four relevant approaches, which have been used to simulate quantum trajectories, in particular, for diffusive continuous measurements. We also performed the calculation of the completeness relation and the unconditioned state update. This is to compare among the four approaches and show the agreement to the expansion of the Lindblad master equation.

Given the existing approaches and their properties, we then proposed a better method, the high-order completely positive map for quantum diffusive weak measurements. The derivation was based on a quantum system coupled to a bosonic bath. We first derived such map in the particular case, where the system's Hamiltonian is $\hat{H} = 0$ and with a single Lindblad operator. We showed that our method can reproduce exactly the Rouchon-Ralph measurement operator, which was obtained from a different intuition (using the classical Euler-Milstein technique). Moreover, the analytical calculation showed that the high-order completely positive map is the most accuracy approach comparing to other approaches. We showed that our mea-

surement operator satisfies the completeness relation and agrees with the Lindblad master equation expansion to the second order in dt. We have also generalised the map to include the system's Hamiltonian $\hat{H}$ and with multiple decoherence channels, separating the measured and the unmeasured channels. In Section 4.3, we showed the two qubit examples, which are the qubit z-measurement, and the measurement of qubit's fluorescence, and derived the high-order completely positive map for both cases. For the qubit z-measurement, we showed that our proposed measurement operator agrees with the expansion of quantum Bayesian approach up to the second order in dt.

In Chapter 5, we made a comparison among four approaches (the Itô map, Rouchon-Ralph approach, quantum Bayesian approach, and our proposed map). We simulated the true measurement records and the true trajectories for $N = 1.5 \times 10^4$, using the Itô approach for a really small time step dt as a benchmark for the comparison. We implemented the coarse graining method to rescale the measurement records to the larger time step dt. Then, we used the coarse records to calculate the quantum trajectories using the four different maps. We investigated the trace distance comparing the generated individual trajectories with the true trajectories and the numerical Lindblad solution. The numerical calculation results showed that our high-order completely positive map $\hat{M}_{\mathrm{W}}$ is the most accurate and precise method. Moreover, we can also confirm with some confidence that the time step d$t = 0.016$ μs used in [20] is a good time resolution, since the least accurate approach, can the Itô approach, still give reasonably small errors.

Bibliography

[1] P. Rouchon and J. F. Ralph, Phys. Rev. A **91**, 012118(2015).

[2] I. A. Gueva and H. M. Wiseman, arXiv:1909.12455.

[3] A. N. Korotkov, Phys. Rev. B **60**, 5737(1999).

[4] A. N. Korotkov, Phys. Rev. B **63**, 115403(2001).

[5] A. N. Korotkov, Phys. Rev. A **65**, 052304(2002).

[6] R. Ruskov and A. N. Korotkov, Phys. Rev. B **67**, 241305(2003).

[7] H. M. Wiseman and G. J. Milburn, *Quantum Measurement and Control* (Cambridge University Press, Cambridge, 2010).

[8] H. J. Carmichael, *An Open Systems Approach to Quantum Optics* (Springer, Berlin, 1993).

[9] C. W. Gardiner, A. S. Parkins, and P. Zoller, Phys. Rev. A **46**, 4363(1992).

[10] M. A. Nielsen and I. L. Chuang, *Quantum Computation and Quantum Information* (Cambridge University Press, Cambridge, 2000).

[11] L. Li, M. J. W. Hall, H. M. Wiseman, Physics Reports **759**, 1-51(2018).

[12] V. P. Belavkin and P. Staszewski, Phys. Rev. A **45**, 1347(1992).

[13] H. M. Wiseman and G. J. Milburn, Phys. Rev. A **47**, 642(1993).

[14] H. M. Wiseman and G. J. Milburn, Phys. Rev. A **47**, 1652(1993).

[15] M. B. Plenio and P. L. Knight, Rev. Mod. Phys. **70**, 101(1998).

[16] J. Steinbach, B. M. Garraway, and P. L. Knight, Phys. Rev. A **51**, 3302(1995).

[17] R. J. Schoelkopf and S. M. Girvin, Nature **451**, 664(2008).

[18] M. Hatridge, S. Shankar, M. Mirrahimi, F. Schackert, K. Geerlings, T. Brecht, K. M. Sliwa, B. Abdo, L. Frunzio, S. M. Girvin, R. J. Schoelkopf, M. H. Devoret, Science **339**, 178(2013).

[19] K. W. Murch, S. J. Weber, C. Macklin, and I. Siddiqi, Nature **502**, 211 (2013).

[20] S. J. Weber, A. Chantasri, J. Dressel, A. N. Jordan, K. W. Murch, and I. Siddiqi, Nature **511**, 570(2014).

[21] P. Campagne-Ibarcq, P. Six, L. Bretheau, A. Sarlette, M. Mirrahimi, P. Rouchon, Phys. Rev. X **6**, 011002(2016).

[22] A. N. Jordan, A. Chantasri, P. Rouchon, B. Huard, Quantum Stud.: Math. Found. **3**, 237(2016).

[23] G.N. Milstein, *Numerical Integration of Stochastic Differential Equations.* (Springer, 1995).

[24] H. Amini, P. Rouchon, and M. Mirrahimi, in *2011 50th IEEE Conference on Decision and Control and European Control Conference* (2011), pp. 8193?8198, ISSN 0191- 2216.

[25] K. Jacobs, Phys. Rev. A **67**, 030301(2003).

[26] I. A. Gueva and H. M. Wiseman, Phys. Rev. Lett, **115**, 180407(2015).

[27] M. Brune, E. Hagley, J. Dreyer, X. Maître, A. Maali, C. Wunderlich, J. M. Raimond, and S. Haroche, Phys. Rev. Lett, **77**, 4887(1996).

[28] G. Lindblad, Commun. Math. Phys. **48**, 119(1976).

[29] A. Chantasri, *Stochastic Path Integral Formalism For Continuous Quantum Measurement* (2016).

[30] C. W. Gardiner, *Handbook of Stochastic Methods: For Physics, Chemistry and the Natural Science* (Springer-Verlag, Berlin, 1985).

[31] H. M. Wiseman, D. W. Utami, H. B. Sun, G. J. Milburn, B. E. Kane, A. Dzurak, and R. G. Clark, Phys. Rev. B **63**, 235308(2001).

[32] A. Chantasri and A. N. Jordan, Phys. Rev. A **92**, 032125(2015).

[33] N. Wonglakhon, S. Suwanna, A. Chantasri, "Euler-Milstein and relevant approaches for high-precision stochastic simulation of quantum trajectories", In Preparation (2020)

Appendices

Appendix A

Euler-Milstein Scheme

In this section, we will show the derivation of the higher order in $\mathrm{d}W$ of the classical stochastic equation. The classical stochastic differential equation can typically be described by

$$\mathrm{d}\vec{x} \;=\; \mathbf{f}(\vec{x}(t),t)\mathrm{d}t + \mathbf{L}(\vec{x}(t),t)\mathrm{d}\vec{W}, \tag{A.1}$$

noting that $\mathbf{L}$ is an arbitrary matrix and $\mathrm{d}W$ is the Wiener increment from stochastic process. Let us integrate over all Eq. (A.1), giving

$$\vec{x}(t) \;=\; \vec{x}(t_0) + \int_{t_0}^{t} \mathbf{f}(\vec{x}(\tau),\tau)\mathrm{d}\tau + \int_{t_0}^{t} \mathbf{L}(\vec{x}(\tau),\tau)\mathrm{d}\vec{W}(\tau). \tag{A.2}$$

Here, we will solve to find the function $\mathbf{f}(\vec{x}(\tau),\tau)$ and $\mathbf{L}(\vec{x}(\tau),\tau)$. We then apply the Itô's lemma, giving

$$\begin{aligned}\mathrm{d}\mathbf{f}(\vec{x}(t),t) = \frac{\partial \mathbf{f}(\vec{x}(t),t)}{\partial t}\mathrm{d}t + \sum_u \frac{\partial \mathbf{f}(\vec{x}(t),t)}{\partial x_u}\mathrm{d}t + \sum_u \frac{\partial \mathbf{f}(\vec{x}(t),t)}{\partial x_u}[\mathbf{L}(\vec{x}(t),t)\mathrm{d}\vec{W}(t)]_u\mathrm{d}t \\ + \frac{1}{2}\sum_{uv} \frac{\partial^2 \mathbf{f}(\vec{x}(t),t)}{\partial x_u \partial x_v}[\mathbf{L}(\vec{x}(t),t)Q\mathbf{L}^{\intercal}(\vec{x}(t),t)]_{uv}\mathrm{d}t,\end{aligned} \tag{A.3}$$

$$\mathrm{d}\mathbf{L}(\vec{x}(t),t) = \frac{\partial \mathbf{L}(\vec{x}(t),t)}{\partial t}\mathrm{d}t + \sum_u \frac{\partial \mathbf{L}(\vec{x}(t),t)}{\partial x_u}\mathrm{d}t + \sum_u \frac{\partial \mathbf{L}(\vec{x}(t),t)}{\partial x_u}[\mathbf{f}_u(\vec{x}(t),t)\mathrm{d}\vec{W}(t)]_u \mathrm{d}t + \frac{1}{2}\sum_{uv} \frac{\partial^2 \mathbf{L}(\vec{x}(t),t)}{\partial x_u \partial x_v}[\mathbf{L}(\vec{x}(t),t)Q\mathbf{L}^\intercal(\vec{x}(t),t)]_{uv}\mathrm{d}t. \quad \text{(A.4)}$$

Let us define the superoperator $\mathcal{L}_t$ as $\mathcal{L}_t \equiv \frac{\partial}{\partial t} + \sum_u \frac{\partial}{\partial x_u} f_u + \frac{1}{2}\sum_{uv} \frac{\partial^2}{\partial x_u \partial x_v}[\mathbf{L}Q\mathbf{L}^\intercal]$ and $\mathcal{L}_{w,v} \equiv \sum_u \frac{\partial}{\partial x_u}\mathbf{L}_{uv}$, giving

$$\mathbf{f}(\vec{x}(t),t) = \mathbf{f}(\vec{x}(t_0),t_0) + \int_{t_0}^{t} \mathcal{L}_t \mathbf{f}(\vec{x}(\tau),\tau)\mathrm{d}\tau + \sum_v \int_{t_0}^{t} \mathcal{L}_{w,t}\mathbf{f}(\vec{x}(\tau),\tau)\mathrm{d}\vec{W}_v(\tau), \quad \text{(A.5)}$$

$$\mathbf{L}(\vec{x}(t),t) = \mathbf{L}(\vec{x}(t_0),t_0) + \int_{t_0}^{t} \mathcal{L}_t \mathbf{f}(\vec{x}(\tau),\tau)\mathrm{d}\tau + \sum_v \int_{t_0}^{t} \mathcal{L}_{w,t}\mathbf{f}(\vec{x}(\tau),\tau)\mathrm{d}\vec{W}_v(\tau). \quad \text{(A.6)}$$

Here, we substitute Eqs. (A.5)-(A.6) to Eq. (A.2), giving

$$\vec{x}(t) = \vec{x}(t_0) + \mathbf{f}(\vec{x}(t_0),t_0)(t-t_0) + \mathbf{L}(\vec{x}(t_0),t_0)(\vec{w}(t)-\vec{w}(t_0)) + \iint \cdots \mathrm{d}\tau\mathrm{d}\tau' + \iint \cdots \mathrm{d}W_v\mathrm{d}\tau + \iint \cdots \mathrm{d}\tau\mathrm{d}W_v + \sum_v \int_{t_0}^{t}\int_{t_0}^{\tau} \mathcal{L}_{w,v}\mathbf{L}(\vec{x}(\tau),\tau)\mathrm{d}W_v\mathrm{d}\vec{W}. \quad \text{(A.7)}$$

We can ignore the high order terms in $\mathrm{d}t$, then

$$\vec{x}(t) = \vec{x}(t_0) + \mathbf{f}(\vec{x}(t_0),t_0)(t-t_0) + \mathbf{L}(\vec{x}(t_0),t_0)(\vec{W}(t)-\vec{W}(t_0)) + \sum_v \int_{t_0}^{t}\int_{t_0}^{\tau} \mathcal{L}_{w,v}\mathbf{L}(\vec{x}(\tau),\tau)\mathrm{d}W_v\mathrm{d}\vec{W}. \quad \text{(A.8)}$$

Let us consider the last term of Eq. (A.8) (setting $\mathrm{d}W_v\mathrm{d}\vec{W} \equiv \Delta\chi_{v,k}$), then at time t_k

$$\sum_v \mathcal{L}_{w,v}\mathbf{L}(\vec{x}(t_k),t_k)\Delta\chi_{v,k} = \sum_v\sum_u \frac{\partial \mathbf{L}_{uv}}{\partial x_u}(\vec{x}(t_k),t_k)\mathbf{L}_{uv}(\vec{x}(t_k),t_k)\Delta\chi_{v,k}. \quad \text{(A.9)}$$

We consider the particular case where $\vec{x}$ is a vector of $1\times m$ ($\because u = 1$),

$$\mathbf{L}(\vec{x}(t),t)\Delta\vec{W} = \sum_{r=1}^{m} \mathbf{L}_r(x(t),t)\mathrm{d}W_r. \quad \text{(A.10)}$$

Then,

$$\sum_v \sum_u \frac{\partial \mathbf{L}_{uv}}{\partial x_u}(\vec{x}(t_k), t_k)\mathbf{L}_{uv}(\vec{x}(t_k), t_k)\Delta\chi_{v,k} = \sum_{v,r} \frac{\partial \mathbf{L}_r}{\partial x}\mathbf{L}_v \Delta\chi_{v,r}, \tag{A.11}$$

$$\begin{aligned}\therefore \vec{x}(t) =& \vec{x}(t_0) + \mathbf{f}(\vec{x}(t_0), t_0)(t - t_0) + \mathbf{L}(\vec{x}(t_0), t_0)(\vec{W}(t) - \vec{W}(t_0)) \\ &+ \sum_{v,r}^{m} \frac{\partial \mathbf{L}_r}{\partial x}\mathbf{L}_v \int_{t_0}^{t}\int_{t_0}^{\tau} \Delta\chi_{v,r}.\end{aligned} \tag{A.12}$$

Now, in the scenario that $v = r$, we can evaluate the integral in Eq. (A.12). We implementing the Itô's lemma by letting $z = x^2, \mu = 0, \sigma = 1, x_0 = 0$,

$$\begin{aligned}\mathrm{d}x &= \cancelto{0}{\mu \mathrm{d}t} + \sigma \mathrm{d}W \\ \mathrm{d}x &= \mathrm{d}W \to x = W \\ \therefore \mathrm{d}x^2 = \mathrm{d}W^2 &= \frac{\partial z}{\partial x}\mathrm{d}x + \frac{1}{2}\frac{\partial^2 z}{\partial x^2}\mathrm{d}x^2 \\ &= 2x\mathrm{d}x + \mathrm{d}x^2 \\ &= 2W\mathrm{d}W + \mathrm{d}W^2\end{aligned} \tag{A.13}$$

$$\therefore \mathrm{d}W^2 = 2W\mathrm{d}W + \mathrm{d}t, \tag{A.14}$$

giving

$$\int_{t_k}^{t_{k+1}}\int_{t_k}^{\tau} \mathrm{d}W(\tau')\mathrm{d}W(\tau) = \int_{t_k}^{t_{k+1}} (W(\tau) - W(t_k))\mathrm{d}W(\tau) \tag{A.15}$$

$$= \frac{\Delta W^2 - \mathrm{d}t}{2}. \tag{A.16}$$

and where $v \neq r$, let $z = x_r x_v$ with $\mu_t = 0, \sigma = 1, x_r(0) = x_v(0) = 0$, we have,

$$\begin{aligned}\mathrm{d}z &= \frac{\partial z}{\partial x_{r,v}}\mathrm{d}x_{r,v} + \frac{1}{2}\frac{\partial^2 z}{\partial x_r \partial x_v}\cancelto{0 (\Delta W_r \Delta W_v = \delta_{r,v}\mathrm{d}t)}{\mathrm{d}x_r \mathrm{d}x_v} \\ \mathrm{d}z &= x_r \mathrm{d}x_v + x_v \mathrm{d}x_r \\ \mathrm{d}(W_r W_v) &= W_r \mathrm{d}W_v + W_v \mathrm{d}W_r.\end{aligned} \tag{A.17}$$

Now, let us consider the last term of Eq. (A.12), we set $\frac{\partial L_r}{\partial x}L_v = \frac{\partial L_v}{\partial x}L_r$ and then rearrange the such equations in this following form,

$$\sum_{r,v} A_r B_v \;\; = \;\; \sum_{r=v} A_r B_s + \sum_{r<v} (A_r B_s + B_s A_r). \tag{A.18}$$

Then we have,

$$\sum_{v,r}^{m} \frac{\partial L_r(x_n)}{\partial x} L_v(x_n) \iint \mathrm{d}W_r(\tau)\mathrm{d}W_s(\tau) = \sum_{r}^{m} \frac{\partial L_r(x_n)}{\partial x} L_r \iint \mathrm{d}W_r(\tau)^2$$
$$+ \sum_{1\le r\le v\le m} \frac{\partial L_v}{\partial x} L_r \int (W_r(\theta) - W_r(t_k))\mathrm{d}W_v(\theta) + (W_v(\theta) - W_v(t_k))\mathrm{d}W_r(\theta). \tag{A.19}$$

Here, the last integral in Eq. (A.19) can be evaluated to $\frac{\Delta W_r \Delta W_v}{2}$, leading to

$$x_{n+1} = x_n + f(x_n)\mathrm{d}t + \sum_{r=1}^{m} L_r(x_n)\Delta W_{r,n}$$
$$+ \sum_{r,v=1}^{m} \frac{\partial L_v(x_n)}{\partial x} L_r(x_n) \left(\frac{\Delta W_{r,n}\Delta W_{v,n} - \delta_{r,v}\mathrm{d}t}{2} \right) \tag{A.20}$$

Appendix B

Quantum Bayesian Approach

This approach, we use the quantum Bayesian conditional probability rule to construct the measurement operator, which is

$$P(X|Y) = \frac{P(Y|X)P(X)}{P(Y)}, \tag{B.1}$$

where $P(X|Y)$ means the probability of getting outcome X if given B.

This section we examine for the two-level system following A. Chantasri's treatment in our notation [29]. Here, we consider a single electron in the double quantum dots. The setting probed the electron by a capacitively coupled quantum point contact. One can detect the current signal which depends on whether the location of the electron is in dot a or b. The system's Hamiltonian of the qubit is $\hat{H} = \frac{\epsilon}{2}\hat{\sigma_z} - \frac{\Delta}{2}\hat{\sigma}_x$ where ϵ is an energy asymmetry between two dot and Δ is a tunnelling rate between two dots. Let us define qubit states $|0\rangle, |1\rangle$ corespond to the two dot locations where r is the measurement readout defined as $r(t) = z(t) + \sqrt{\tau}\xi(t) = y_t/\sqrt{\tau}$. We also define a 2×2 density matrix as $\rho = \{\{\rho_{00}, \rho_{01}\}, \{\rho_{10}, \rho_{11}\}\}$. We can write the probability of the state being in $|0\rangle$ given the measurement outcome r as

$$P(0|r) = \frac{P(r|0)}{\rho_{00}P(r|0) + \rho_{11}P(r|1)}, \tag{B.2}$$

here we have used $P(0) = \rho_{00}$ and $P(1) = \rho_{11}$, we can do in the same way for

the state $|1\rangle$. From the central limit theorem, the probability distributions for the measurement readout r are given by

$$P(r|0) = \sqrt{\frac{\mathrm{d}t}{2\pi\tau}}\exp\left[-(r-1)^2\frac{\mathrm{d}t}{2\tau}\right], \tag{B.3}$$

$$P(r|1) = \sqrt{\frac{\mathrm{d}t}{2\pi\tau}}\exp\left[-(r+1)^2\frac{\mathrm{d}t}{2\tau}\right]. \tag{B.4}$$

We can write the measurement operator by using quantum Bayesian update, which is

$$\begin{aligned}\hat{M}_r &= \sqrt{P(r|0)}\,|0\rangle\langle 0| + \sqrt{P(r|1)}\,|1\rangle\langle 1|\,, \\ &= \left(\frac{\mathrm{d}t}{2\pi\tau}\right)^{1/4}\exp\left[-\frac{\mathrm{d}t(r-\hat{\sigma}_z)^2}{4\tau}\right]\end{aligned} \tag{B.5}$$

Since we consider imperfect measurements, we can think of the losing information as averaging all possible lost readouts, which is

$$\mathcal{O}_\gamma = \int \mathrm{d}r_u \hat{M}_{r_u}\rho\hat{M}_{r_u}^\dagger, \tag{B.6}$$

where we call it a dephasing term and operate this on the off-diagonal elements of ρ. The state update evolution of qubit is given by

$$\rho(t+\mathrm{d}t) = \mathcal{O}_\gamma\mathcal{U}_{\delta t}\mathcal{M}_{r_n}[\rho(t)], \tag{B.7}$$

where $\mathcal{U}_{\delta t}[\rho(t)] = e^{-i\hat{H}\delta t}\rho(t)e^{i\hat{H}\delta t}$ is a unitary operation and $\mathcal{M}_{r_n}[\rho(t)] = \frac{\hat{M}_{r_n}\rho(t)\hat{M}_{r_n}^\dagger}{\mathrm{Tr}\left(\hat{M}_{r_n}\rho(t)\hat{M}_{r_n}^\dagger\right)}$.